

Pyramids of Life: A Size Spectrum Model of the Southwestern UK Marine Ecosystem

Kaitlyn Louth

Supervisors: Prof Jon Pitchford
Dr Murray Thompson

May 2022

A dissertation submitted in partial fulfillment of the requirements for the degree of
Master of Mathematics (MMath)



Department of Mathematics, University of York
in collaboration with
The UK Centre for Environment, Fisheries and Aquaculture Science (Cefas)

Abstract

The mathematical idea behind size spectrum theory is that the abundance or biomass of organisms are described as a function of body size. This is a useful model system in the context of marine species because predators are mostly limited by the size of their mouths, therefore predation is driven by body size [1, 2]. Size spectra can be calculated if we know the growth rate, reproduction, and the mortality of individuals as a function of body size. This report outlines the motivations for using multispecies size spectrum modelling and the mathematics that underpins this. We parameterise a multispecies model for the ecosystem off the Southwest coast of the UK, and calibrate it to the current ecosystem by utilising data and insight provided by Cefas. We use the R package `mizer` to set up the model and run simulations. By understanding the dynamics obtained from size spectra simulations, we can develop an intuition of how marine ecosystems behave and how to maintain sustainability within an ecosystem. The different fishing regimes that we explore and simulate are: constant fishing effort at minimum landing size, a system without fishing, and balanced harvesting. Balanced harvesting is the idea that we distribute fishing mortality across species and size, in line with productivity [3]. By comparing the slopes and shape of biomass spectra and plots of biomass varying over time, we find that balanced harvesting results in the highest yield whilst also not greatly affecting biomass structure, suggesting it could be a sustainable fishing method.

Acknowledgements

Thank you to my supervisor Jon Pitchford for his excellent insight and advice throughout the project, and to Murray Thompson at Cefas for supplying the data sources and providing insight on these. Also a special thanks to Gustav Delius for his guidance in using `mizer`, and Kennedy Osuka for his useful comments. All of whom are researchers on the ‘Pyramids of Life: Working with Nature for a Sustainable Future’ project.

Contents

1	Introduction	3
1.1	Why is this Research Important?	3
1.2	Project Aims and Objectives	5
2	What is a Size Spectrum?	5
2.1	Representations of Size Spectra	6
2.2	Size Spectrum Modelling Frameworks	9
3	Size Spectrum Dynamics	10
3.1	McKendrick-von-Foerster Equation	10
3.2	von Bertalanffy Growth Model	12
3.3	Mortality	13
3.3.1	Predation	13
3.3.2	Fishing Mortality	16
3.4	Reproduction & Somatic Growth	17
3.5	Steady State Solution of the McKendrick-von-Foerster Equation	18
4	Implementing the Multispecies Model	21
4.1	Introducing <code>mizer</code>	21
4.2	Multispecies Model Data	22
4.2.1	Data Pre-Processing & Data Assumptions	23
5	Results	25
6	Discussion	35
7	Conclusion	37
References		38
A	Compiled List of Original Model Parameters	42
B	Species Interaction Matrix	43
C	Code to Extract the Observed Biomass	44
C.1	Time Series of Arithmetic Average Biomass Density	47
C.2	Time Series of Geometric Average Biomass Density	48
C.3	Observed Biomass Parameters using Arithmetic Mean	49
D	Code to Create a Multispecies Size Spectrum Model using <code>mizer</code>	49
D.1	R Shiny Tuning Parameters Gadget	56
D.2	Tuning Growth Curves	57

1 Introduction

1.1 Why is this Research Important?

Currently nearly 90% [4] of the world's marine fish stocks are fully exploited, over-exploited or depleted, therefore it is crucial to understand how the relationships between different fish species and their ecosystem, are intertwined with human demand for fish and fishing pressure. This is the focus of a large, collaborative research project called 'Pyramids of Life: Working with Nature for a Sustainable Future' [5], which aims to identify where changes need to be made to fisheries management so that marine ecosystems can be ecologically sustainable. The anticipated conclusions from this project therefore have national and even global outreach and implications. This is vital research today because in the SOFIA report (2020), the U.N. states that fish consumption has been outpacing both the world population expansion rate since 1961 and the meat consumption rise [6]. The report goes on to say that since 1961, global fish consumption has risen from 9.0 kg per capita to 20.3 kg in 2017, providing approximately 3.3 billion people with almost 20% of their average per capita intake of animal protein [6].

Consequently, demand for large commercial fish such as cod has increased such that the pyramids of biomass for marine ecosystems are being over-exploited at the highest trophic levels. This is unsustainable because we are depleting predator populations and reducing biodiversity, meaning marine ecosystems are vulnerable to disruption and food supply is threatened. The basis of this 'Pyramids of Life' wider project is to transform the current unsustainable pyramids of biomass into a healthy ecosystem, through trying to equally exploit all the different sized categories within the ecosystem. These categories are obtained from individual-level data across different species. Figures 1-3 are based on figures from the Pyramids of Life research proposal submitted to the Sustainable Management of UK Marine Resources (SMMR) research programme [5]. They represent these types of sustainable and unsustainable pyramids and show how fishing pressure affects biomass structure [5].

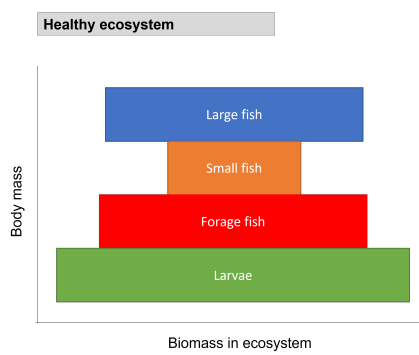


Figure 1: Schematic pyramid showing the relative proportions of biomass in a healthy marine ecosystem for different fish size groups/trophic levels.

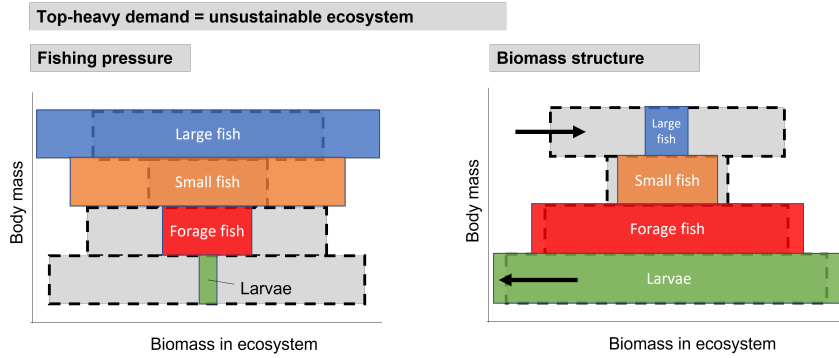


Figure 2: Schematic pyramids showing the relative proportions of biomass we currently fish, and the effect that the current fishing pressure on larger fish species has on these proportions of biomass in an ecosystem, for different fish size groups/trophic levels.

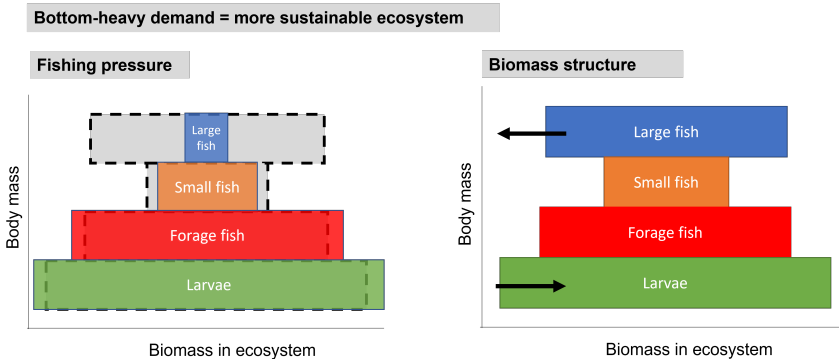


Figure 3: Schematic pyramids showing the relative proportions of biomass that would be fished using bottom-heavy fishing pressure, and the effect that would have on biomass structure, for different fish size groups/trophic levels.

One of the deliverables that the 'Pyramids of Life' project hopes to achieve is to 'identify changes in management, including tuning fishing gear and modulations in effort, which can achieve the desired ecosystem-level changes' [5]. This will involve modelling and simulating marine ecosystems under different fishing gears, fishing pressure and fishing effort to determine which changes in management and fishing strategy could result in a more sustainable ecosystem. This is important because we need to find new ways to harvest marine ecosystems that reduce human impacts on them, and improve their sustainability and resilience to climate change [5].

1.2 Project Aims and Objectives

The primary aim of this project is to parameterise a multispecies model for the marine ecosystem off of the Southwest coast of the UK, and calibrate it to the current ecosystem using Cefas ecological and catch data. This area provides our focus because there exists a mixed demersal fishery there, meaning it can only target rather than precisely control their fishing effort [7]. Consequently, this means that mixed-species catches are more difficult to minimise. The multispecies modelling framework will allow for altering species specific parameters, hence observing how a change in one species will affect the ecosystem as a whole. The species of interest as outlined in the Pyramids of Life research proposal are: hake, whiting, haddock, cod, saithe, ling, anglerfish, megrim, sole, and plaice. The secondary aim of this project is to learn how the Southwestern UK marine ecosystem will function under different fishing regimes, namely: constant fishing at species' minimum landing size, an ecosystem without fishing, and balanced harvesting. This will be achieved by projecting simulations of the multispecies model forward in time.

The model will be based on the mathematics of multispecies size spectra dynamics. This will consist of systems of coupled partial differential equations that track body-size distributions of individual species over time. Size spectrum models follow the general principle that larger organisms eat smaller ones [2], and therefore increase in size accordingly. Through use of the R package `mizer` (multi-species size spectrum modelling in R) [8], we will use numerical solutions of the mathematical model to simulate and investigate biomass spectra, and how biomasses of species vary over time when different fishing scenarios are implemented. We hope to draw some conclusions into how the current marine ecosystem in the Southwest of the UK can be more sustainably fished.

The structure of this report is therefore as follows. Section 2 defines size spectra, describes how size spectra are represented and discusses multiple size spectrum modelling frameworks. Section 3 introduces the mathematics which underpin size spectrum dynamics, such as the growth and mortality rates. Additionally within this section, we define the fishing methods which we implement in our simulations (see 3.3.2 Fishing Mortality). Section 4 introduces how the R package `mizer` can be used to set up and run simulations of a multispecies size spectrum model, and discusses the data sources used to parameterise such a model. This includes descriptions of data pre-processing and data assumptions. In Sections 5 and 6 we present the results of our simulations, for example plots of biomass spectra and plots of biomass over time, and draw conclusions from such results.

2 What is a Size Spectrum?

Traditional fisheries management is based on species and total biomass, paying limited or no attention to size structure. For example, maximum sustainable yield (MSY) is a single-species approach which takes the largest average catch that can be captured from a stock. However, there is evidence that these approaches fail because they do not take into

consideration the effect of fishing on the entire ecosystem, therefore resulting in a continued trajectory of decline for most species [9]. It is therefore becoming increasingly important to base fisheries management on size structure too. The term ‘size spectrum’ was coined in the 1960s by Sheldon and Parsons [10] to describe the relationship between abundance and body size. They proposed that size spectra could be used to discover patterns in plankton communities, and this acted as a catalyst for further research into this relationship. It was observed that in marine ecosystems there is a power-law relationship between abundance and body size, where individuals are only described by their body size without any reference to their taxa [11]. The relevance and attraction for modelling marine ecosystems using body size as the only trait, is based on the evidence that numerous ecological processes such as growth rate, metabolic rate and population abundance all correlate strongly with body size [12]. Additionally with regard to fishing, body size is a useful measurement to define fishing gear regulations, and the regularity of size spectra distributions means that any deviations can be used to characterise the impacts of fishing on an ecosystem [13]. Therefore, size spectrum models are emerging as a championed alternative to modelling large systems of individuals that grow and change trophic level during their lifetime. We can formalise these ideas with some definitions.

Definition 2.1. The **abundance** N of a size group is measured as the number of individuals per size group. It represents the balance between how many individuals grow into the group, how many grow out of it, and how many are dying in that group [14].

Definition 2.2. The **biomass** B of a size group is the average mass of all living species within a size range. It is measured as the average mass of a species per unit area (typically kg/km^2 for marine species).

Definition 2.3. The **size spectrum** represents abundance or biomass of individuals as a function of their body size. It is typically expressed as a frequency distribution on a logarithmic scale of abundance and body size.

Note that in this context, body size refers to body mass [13]. Additionally, ‘size group’ will be discussed more rigorously in Section 3.

2.1 Representations of Size Spectra

There are three types of size spectra that are commonly used in the literature; the abundance density spectrum $N(w)$, the biomass density spectrum $B(w)$, and the Sheldon spectrum $B^{Sheldon}(w)$ [13]. (Note that these are all represented as functions of body size w). We can create the biomass density spectrum by multiplying the abundance density spectrum by body size, and then further create the Sheldon spectrum by multiplying the biomass density spectrum by body size:

$$N(w) = \frac{B(w)}{w} = \frac{B^{Sheldon}(w)}{w^2}. \quad (1)$$

Hence, we can show that the biomass density spectrum is equivalent to the abundance of individuals as a function of log size, and the Sheldon spectrum is equivalent to the biomass of individuals as a function of log size. If we want to find the abundance of fish between sizes w_1 and w_2 , we would integrate the abundance density spectrum between our size range with respect to body size

$$\mathcal{N} = \int_{w_1}^{w_2} N(w) dw. \quad (2)$$

If we then convert our size scale to log size, such that we want to find the abundance of fish between log sizes x_1 and x_2 , we would solve a new integral over the abundance density spectrum as a function of log size between our log size range.

$$\mathcal{N} = \int_{x_1}^{x_2} N(x) dx. \quad (3)$$

This abundance will still be equivalent to the abundance in Equation 2. Let us now show how we can write Equation 2 in log scale using the change of variable

$$x = \ln(w) \implies w = e^x.$$

Taking the derivative of w with respect to x , we get

$$\frac{dw}{dx} = e^x \implies dw = e^x dx.$$

Finally to convert the limits in Equation 2 to log scale, we substitute them into $x = \ln(w)$ such that

$$\begin{aligned} w = w_1 &\implies x = \ln(w_1) \\ w = w_2 &\implies x = \ln(w_2). \end{aligned}$$

Substituting this into Equation 2, we obtain

$$\begin{aligned} \mathcal{N} &= \int_{\ln(w_1)}^{\ln(w_2)} N(e^x)e^x dx \\ &= \int_{x_1}^{x_2} N(w)w dx. \end{aligned} \quad (4)$$

Now by a direct comparison of Equation 3 with Equation 4, we have

$$\begin{aligned} N(x) &= N(w)w \\ \implies N(\ln(w)) &= N(w)w = B(w). \end{aligned}$$

Therefore, we have shown that abundance as a function of log size is equivalent to biomass as a function of size. Similarly, following this same method we would see that biomass as a function of log size is equivalent to the Sheldon spectrum as a function of size, i.e.

$$B(\ln(w)) = B(w)w = B^{Sheldon}(w).$$

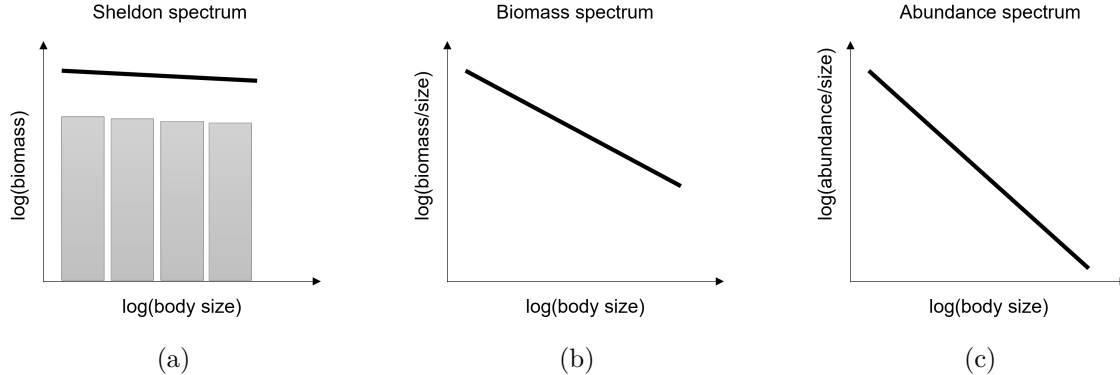


Figure 4: Three representations of size spectra: the Sheldon spectrum, the biomass spectrum, and the abundance spectrum. (Image inspired by Andersen (2019) [14]).

These spectra can therefore be characterised by

$$N(w) w^p = \begin{cases} \text{abundance spectrum} & \text{if } p = 0 \\ \text{biomass spectrum} & \text{if } p = 1 \\ \text{Sheldon spectrum} & \text{if } p = 2. \end{cases} \quad (5)$$

If data tells us that there exists a power-law relationship between biomass/abundance and size, then the size spectra in Figure 4 can be approximated with power-law functions such that [14]:

$$\begin{aligned} N(w) &= K w^{-\lambda} \\ B(w) &= K w^{1-\lambda} \\ B^{Sheldon}(w) &= K w^{2-\lambda}, \end{aligned} \quad (6)$$

where K is the spectrum coefficient and λ is the spectrum *slope*. These power-law distributions were initially observed shortly after ‘size spectrum’ was first coined, in the 1972 work of Sheldon et al. [15], whom realised there is a negative power-law relationship between abundance and body size when sampling size distributions of plankton [1]. This relationship is represented by the shape of the abundance spectrum (Figure 4c), and agrees with the notion that in marine ecosystems where growth across several size classes can occur and where predators are generally larger than prey, most individuals are eaten before they become particularly large [16]. This results in a decline in abundance as body size increases. Since Sheldon’s discovery, this negative power-law relationship has also been observed over different size ranges, from phytoplankton up to large fish [1, 11], indicating that large individuals in marine ecosystems are far more rare.

Sheldon et al. (1972) additionally established that in their plankton sample there were approximately equivalent abundances of biomass in logarithmically increasing size brackets

[1, 11]. This coincides with the Sheldon spectrum in Figure 4a, which is represented as a histogram of biomass in logarithmically equal body size intervals [14]. We can see that biomass is approximately invariant over logarithmically equal body size intervals, meaning it is independent of body size [16]. However, this does not provide the most convenient representation of biomass in an ecosystem, because the level of biomass in each interval is dependent on the interval size. This made it difficult to compare levels of biomass in different publications, because different body size intervals were used. The abundance and biomass spectra are independent of size intervals, and are therefore now more preferable in the literature.

A general feature of the biomass size spectrum is that it has an exponent close to -1, which stems from this notion that biomass is independent of body size. This is because if the Sheldon spectrum is approximately flat, the exponent in Equation 6 is nearly equal to zero, which implies $\lambda \approx 2$. Then substituting $\lambda \approx 2$ into the other power-law functions in Equation 6, means that the biomass spectrum has an approximate exponent of -1 , and the abundance spectrum an exponent around -2 .

2.2 Size Spectrum Modelling Frameworks

In general there are three types of size spectrum modelling frameworks of decreasing levels of complexity: the multispecies size spectrum model, the trait-based size spectrum model, and the community size spectrum model. Both the trait-based and community models can be considered as direct simplifications of the most complex framework, the multispecies model. This framework represents individual populations with species-specific parameters and prey preferences, such that multiple species are resolved [13]. For example, species-specific life-history parameters will exist, there will be different fishing gear selectivity targeting different species size groups, the fishing effort of each gear will vary over time rather than being constant, and the species-species interactions will be taken into account too [8]. Fishing mortality is discussed thoroughly in Section 3.3.2, where terminology such as ‘gear selectivity’ is defined.

The trait-based model is a simplified version of the multispecies model, because it reduces the differences among species to only a single continuous variable/trait, which is typically the asymptotic size or equivalently the maturation size [13]. It is derived from the multispecies model by assuming that all of the species-specific parameters such as predator-prey ratio and size preference are the same for all species. Other features of this framework is that the number of species does not affect the general spectrum dynamics, and the asymptotic sizes of the species are evenly distributed over the community size range [8]. The solution is the trait size spectrum, which describes the joint distribution of individual and asymptotic sizes. In numerical analyses, the asymptotic size axis is grouped into logarithmically spaced asymptotic size classes.

Finally, the trait-based model can be further simplified to give the community size spectrum modelling framework. In this framework, all of the differences among species are ignored,

hence representing a single population of individuals that differ only by body size. This means that only one species is resolved. It can be derived by summing over the number of different species i [17]:

$$N_c(w) = \sum_{i=1} N_i(w).$$

One of the significant differences between this model and the trait-based model is that in a community model, maturation and reproduction is not considered, so recruitment is constant and there is no relationship between the abundance in the community and egg production [8]. Recruitment is the rate at which individuals become available to a fishery after surviving the early life stages [14].-

3 Size Spectrum Dynamics

We shall focus on the multispecies spectrum modelling framework. Size spectrum dynamics describe the flow of biomass through an ecosystem across different trophic levels. It can be useful to think of traffic flow dynamics to understand the theory behind size spectrum dynamics. For example, the flow of traffic on the motorway is dependent on the traffic density, which is in turn dependent on changes in traffic velocity. Therefore, traffic jams occur when there is a decrease in velocity somewhere causing the density of cars to increase, then this results in a further decrease in speed, leading to an even higher density, and so on. To avoid these peaks in high traffic density, smart motorways are being introduced in the UK, which use variable speed limits and open up the hard shoulder to control the flow of traffic [18]. Regarding marine ecosystems, high fish density occurs in trophic levels where the growth rate decreases, and so we want to avoid pronounced peaks in fish density in a similar way that we want to avoid high peaks in traffic density. For example, we are seeing stunted growth of cod in the Baltic Sea due to the depletion of its benthic prey as a result of increased hypoxia [19]. Furthermore, we would need to consider growth dynamics too i.e. general flow across the trophic levels. We can try to influence the size spectrum dynamics of a marine ecosystem through fishing policy and help resolve the issue in the Baltic Sea, such as by reducing cod numbers (and in turn increasing their growth rate due to fewer competitors for food), or reduce fishing on their prey [20]. Changes in these size spectrum dynamics are as a result of changes to the abundance of different size groups that individuals are categorised into.

Therefore, size-spectrum dynamics are a consequence of the balance, or lack thereof, between the death rate and the changes in the growth rate. This interaction can be described by the McKendrick-von-Foerster equation.

3.1 McKendrick-von-Foerster Equation

The McKendrick-von-Foerster (MvF) equation [21, 22] is a partial differential equation (PDE) which formalises the balances that determine the abundance of a size group, as

described in Definition 2.1:

$$\frac{\partial N_i(w)}{\partial t} + \frac{\partial(g_i(w)N_i(w))}{\partial w} = -\mu_i(w)N_i(w). \quad (7)$$

Here, $g_i(w)$ is the growth rate of individuals with weight w and $\mu_i(w)$ is the individual death rate, and these are determined by food availability, predation and fishing mortality [8]. $N_i(w)$ is the individual-level abundance size spectrum (numbers per unit weight) for species i .

The MvF equation can be derived if we consider the increase and decrease of individuals in the body size range $w \pm \frac{\Delta w}{2}$. The number of individuals within that size range is approximately equal to $N_i(w)\Delta w$. We define $flux_{(in)}$ as the rate at which smaller individuals grow into our body size range, and similarly define $flux_{(out)}$ as the rate at which individuals grow out of our range and into a bigger size class. So for a short time interval, Δt , the flux into and out of our range is the growth rate multiplied by the abundance at the boundary and the time interval:

$$flux_{(in)} = g_i\left(w - \frac{\Delta w}{2}\right)N_i\left(w - \frac{\Delta w}{2}\right)\Delta t, \quad (8)$$

$$flux_{(out)} = g_i\left(w + \frac{\Delta w}{2}\right)N_i\left(w + \frac{\Delta w}{2}\right)\Delta t. \quad (9)$$

The flux of individuals disappearing from the group is the number of deceased individuals in our time interval, which we define as $flux_{(deceased)}$. It is approximated by the total number of individuals in the size range, multiplied by the death rate and the time interval:

$$flux_{(deceased)} = \mu_i(w)N_i(w)\Delta w\Delta t. \quad (10)$$

Then by combining Equations 8-10, we obtain the total change in the number of individuals within our size class

$$\begin{aligned} \Delta N_i \Delta w &= flux_{(in)} - flux_{(out)} - flux_{(deceased)} \\ &= g_i\left(w - \frac{\Delta w}{2}\right)N_i\left(w - \frac{\Delta w}{2}\right)\Delta t - g_i\left(w + \frac{\Delta w}{2}\right)N_i\left(w + \frac{\Delta w}{2}\right)\Delta t \\ &\quad - \mu_i(w)N_i(w)\Delta w\Delta t. \end{aligned} \quad (11)$$

Since our size range is small, we can approximate the growth rate at $w \pm \frac{\Delta w}{2}$ by a linear expansion, such that $g_i(w \pm \Delta w/2) \approx g_i(w) \pm g'_i(w)\Delta w/2$. Likewise, $N_i(w \pm \Delta w/2) \approx N_i(w) \pm g'_i(w)\Delta w/2$. By substituting these into Equation 11 and simplifying, we obtain

$$\frac{\Delta N_i}{\Delta t} = -g'_i(w)N_i(w) - N'_i(w)g_i(w) - \mu_i(w)N_i(w). \quad (12)$$

Note that $g'_i(w)N_i(w) + N'_i(w)g_i(w)$ is equivalent to $\partial(g_i(w)N_i(w))/\partial w$, so substituting this into Equation 12 we obtain

$$\frac{\Delta N_i}{\Delta t} = -\left(\frac{\partial(g_i(w)N_i(w))}{\partial w}\right) - \mu_i(w)N_i(w), \quad (13)$$

and taking the limit of Equation 12 as $\Delta t \rightarrow 0$ results in the MvF equation (Equation 7).

The MvF equation is also accompanied by a boundary condition at the boundary $w = w_0$, such that the $flux_{(in)}$ is determined by the reproduction of offspring by individuals at maturity, R_i :

$$flux_{(in)}(w_0) = g_i(w_0)N_i(w_0) = R_i. \quad (14)$$

We need to define the growth and mortality functions which can be incorporated into the MvF equation.

3.2 von Bertalanffy Growth Model

The growth rate we will consider within the MvF equation is described by the von Bertalanffy growth model, which is an overall individual growth rate dw/dt involving two processes [23]:

$$\frac{dw}{dt} = Aw^n - kw. \quad (15)$$

These two processes represent acquisition of energy Aw^n and losses kw , where the exponents n and 1 describe how the processes scale with size. Since these exponents are different, the processes will not be proportional to each other. For example, at some size W_∞ , all of the energy will be used for losses and growth will stop. We define this size as the asymptotic weight/size of an individual. Therefore, by setting Equation 15 to zero we can obtain W_∞ :

$$W_\infty = \left(\frac{A}{k}\right)^{\frac{1}{(1-n)}}. \quad (16)$$

This establishes that there exists some relationship between A and k that determines asymptotic size, such that large species either acquire more energy or have smaller losses. Therefore, the differences in growth between species can be defined solely on their asymptotic size and growth coefficient A [14]. So equation 15 can be rewritten as [23]

$$\frac{dw}{dt} = Aw^n \left[1 - \left(\frac{w}{W_\infty}\right)^{1-n}\right] = g(w). \quad (17)$$

The growth coefficient A describes processes that are related to energy acquisition and assimilation, and we can find its value by deriving the relationship between A and the von Bertalanffy parameters [14]. von Bertalanffy argued that acquisition was limited by processes which involve absorbing food across a surface (i.e. a digestive system), and fish

in particular are limited by ‘the simple surface rule’ [23]. This states that the surface of an organism is proportional to $w^{\frac{2}{3}}$. The standard relation between weight w and length l is $w = cl^3$, where c is the length-weight coefficient ($c \approx 0.001$). Using this alongside the simple surface rule, we can rewrite Equation 15 in length-based form

$$\begin{aligned} \frac{dl}{dt} &= K(L_\infty - l) \\ \implies l(t) &= L_\infty(1 - e^{-Kt}), \end{aligned} \tag{18}$$

where L_∞ is the asymptotic length and K is the von Bertalanffy growth constant

$$K = \frac{A}{3c^{\frac{1}{3}}} \frac{1}{L_\infty} \text{ for } n = \frac{2}{3}. \tag{19}$$

In Section 4, when it comes to implementing our multispecies model, A is found using Equation 19 by inputting the two von Bertalanffy parameters (or asymptotic weight W_∞) from empirical data.

3.3 Mortality

3.3.1 Predation

The primary cause of mortality in marine ecosystems is predation, because it is extremely rare that marine organisms will naturally die from old age, instead they will be eaten by larger predators [14]. To derive predation mortality we need to consider: the size of prey that predators prefer to eat, the predator-prey encounter rate, the prey consumption rate, and search volume. Primarily, the size preference of prey may be different from the sizes of prey that a predator has eaten when analysing stomach content data, because we know from Figure 4a that biomass of prey is approximately independent of size - smaller prey are more abundant than larger prey. Ursin (1973) described the preference for prey weight in the form of a log-normal selection model [24], which represents prey preference in terms of the ratio between the weight of predators w and the weight of prey w_p

$$\phi(w, w_p) = \exp\left[\frac{-(\ln(w/(\beta w_p)))^2}{2\sigma^2}\right], \tag{20}$$

where β is the preferred predator-prey mass ratio and σ is the width of the size selection function. Ursin was able to show that the preferred predator-prey mass ratio was generally smaller than the predator-prey size ratio of prey in stomach contents of cod and dab [14, 24].

The availability of prey $E_a(w)$ can be represented by the integral over a resource spectrum $N_{\text{res}}(w_p)$ and an abundance density spectrum of prey species $N(w_p)$ (units of number per mass per volume), weighted by prey size preference

$$E_a(w) = \int_0^\infty (N(w_p) + N_{\text{res}}(w_p)) w_p \phi(w, w_p) dw_p, \tag{21}$$

where $E_a(w)$ has units mass per volume. The resource spectrum is representative of the background food items available for the smallest individuals in the ecosystem (smaller than βw_0) [8]. Then the predator-prey encounter rate $E(w)$ is dependent on the prey availability as well as the search volume, which is assumed to scale with individual weight and described as a power law:

$$V(w) = \gamma w^q. \quad (22)$$

Therefore, the predator-prey encounter rate can be written as the prey availability multiplied by the search volume:

$$\begin{aligned} E(w) &= \gamma w^q E_a(w) \\ &= \gamma w^q \int_0^\infty (N(w_p) + N_{\text{res}}(w_p)) w_p \phi(w, w_p) dw_p. \end{aligned} \quad (23)$$

Not all the encountered prey are consumed because individuals have a maximum consumption rate dependent on their size

$$h(w) = hw^n. \quad (24)$$

Therefore, if $E(w) > hw^n$, the consumption is subject to a Holling Type II functional response that represents satiation [8]

$$f(w) = \frac{E(w)}{E(w) + hw^n}. \quad (25)$$

We call $f(w)$ the feeding level, and it varies between 0 and 1 such that when $E(w) \ll hw^n$, then the feeding level is proportional to the encountered prey (i.e. all encountered prey are consumed), and when $E(w) \gg hw^n$, the feeding level approaches 1 [14]. This implies that $1 - f(w)$ is the proportion of the encountered food that is consumed, and therefore the rate at which food is consumed is

$$\text{consumption} = f(w)hw^n. \quad (26)$$

For simplicity, we will use the assumption that the resource spectrum is always at its carrying capacity, therefore Equation 23 can be rewritten as

$$B^{\text{prey}}(w) = \int_0^\infty N(w_p) w_p \phi(w, w_p) dw_p, \quad (27)$$

which represents the biomass of encountered prey. Substituting in the power-law form for the abundance spectrum, $N(w_p) = Kw_p^{-\lambda}$, the integral can be solved to obtain

$$B^{\text{prey}}(w) = \Phi K w^{2-\lambda}, \quad (28)$$

where

$$\Phi = \sqrt{2\pi} \sigma \beta^{\lambda-2} \exp[(\lambda-2)^2 \sigma^2 / 2] = \text{constant}.$$

Note that Φ involves the parameters which are also in the predator-prey preference function (see Equation 20). The predation mortality is then calculated such that everything that is eaten translates into corresponding predation on the ingested prey individuals [8]. Using the notion that $1 - f(w)$ is the proportion of the food encountered by a predator that is actually consumed, the rate at which predators consume prey of size w_p is

$$\begin{aligned}\mu_p(w_p) &= \int_0^\infty N(w)V(w)\phi(w, w_p)(1 - f(w)) dw \\ &= \int_0^\infty Kw^{-\lambda}\gamma w^q\phi(w, w_p)(1 - f(w)) dw,\end{aligned}\tag{29}$$

where μ_p is the predation mortality.

We can further simplify this by using the same assumptions made by Armstrong and Schindler (2011), whom used an average feeding level f_0 which is large enough to satisfy metabolism, yet also small enough to reflect that fish with full stomachs are rarely caught [25]. We can now rewrite consumption as this factor f_0 multiplied by the maximum consumption (Equation 24)

$$\text{consumption} = f_0 hw^n.\tag{30}$$

Then if we consider the relationship between consumption, biomass of encountered prey and search volume as expressed by Andersen and Beyer (2006) [26]

$$B^{\text{prey}} = \frac{\text{consumption}}{V},$$

we can substitute Equations 22, 28 and 30 into this expression and isolate the size spectrum:

$$\begin{aligned}\Phi Kw^{2-\lambda} &= \frac{f_0 hw^n}{\gamma w^q} \\ \implies Kw^{-\lambda}\Phi w^2 &= \frac{f_0}{\gamma} hw^{n-q} \\ \implies Kw^{-\lambda} &= N(w) = \frac{f_0}{\gamma} \frac{h}{\Phi} w^{n-q-2}.\end{aligned}\tag{31}$$

Finally inserting this size spectrum solution into a revised expression for the predation mortality, which takes into account the Armstrong and Schindler assumption

$$\mu_p(w_p) = \int_0^\infty V(w)N(w)\phi(w, w_p) dw\tag{32}$$

gives

$$\mu_p(w) = \Phi_p f_0 hw^{n-1}, \text{ with } \Phi_p = \beta^{2n-q-1} e^{(2n-q-1)(q-1)\sigma^2/2} = \text{constant.}\tag{33}$$

3.3.2 Fishing Mortality

In this subsection we explain two established fishing concepts which have a long history in fisheries management, which utilise internationally agreed metrics for fishing mortality. Firstly, fishing mortality can be imposed on fish by fishing gears which catch species within a particular size range. The size range is described by the gears' selectivity $S_i(w)$, for example beam trawls catch anything large enough not to slip through the net. Then to obtain the fishing mortality on a stock (an exploited population), the gear selectivity is multiplied by the catchability by species C_i and the fishing effort ϵ

$$\mu_{f,i}(w) = S_i(w)C_i\epsilon. \quad (34)$$

The catchability is a measure of the proportion of species i that is removed by 1 unit of fishing effort [27], where fishing effort is the amount of fishing gear of a specific type used on the fishing grounds over a given unit of time. In this way effort can then be specified relative to a 'base effort' [8]. The gear selectivity is described by a selectivity function, and we shall focus on knife-edge selectivity. Knife-edge selectivity prescribes a sudden change of selectivity from 0 to 1 at a particular size for each species. The landings data we will use to implement a multispecies size spectrum model are mostly caught using beam trawls, the selectivity of which is a sigmoidal function

$$S_{\text{beam}} = \left[1 + \left(\frac{w}{w_S} \right)^{-u} \right]^{-1}. \quad (35)$$

If $u \rightarrow \infty$ we have knife-edge selectivity, and then w_S would be the knife-edge size, which is the point of the sudden change. For example in Figure 5, we see this change at size 25cm i.e. $w_S = 25$. Each gear has the same selectivity function for all the species it selects, however the parameter values for each species may be different. For example, the knife-edge size for each species is likely to be different.

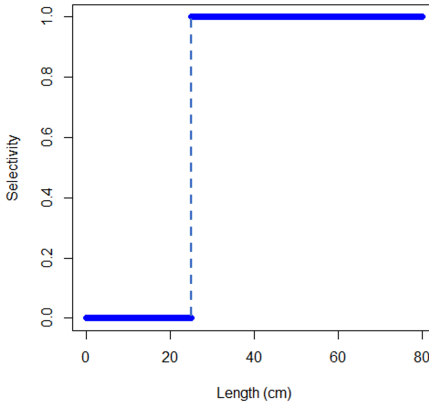


Figure 5: Example of knife-edge selectivity of a beam trawl on a species of fish, where $w_S = 25$ is the minimum length of species that the gear selects.

Alternatively, fishing mortality can be imposed on a system in terms of balanced harvesting. In Garcia *et al.* (2012), balanced harvesting was initially described as distributing mortality from fishing across the widest possible range of species, stocks, and sizes in an ecosystem [3]. Furthermore, it was explained to be a fishing method that adjusts fishing mortality in line with the productivity based on an individual's species and size [3]. Law & Plank (2018) later defined balanced harvesting such that fishing mortality is proportional to the rate of somatic production [28]. By somatic production, they mean that only the remaining energy after assimilation is considered when assessing an individual's productivity. Law & Plank calculated the rate of somatic production as

$$\mathcal{P}_i(x, t) = \epsilon_i(x, t)s_i(x, t)u_i(x, t)w_0e^x, \quad (36)$$

where $\epsilon_i(x, t)$ is the proportion of consumed biomass used for individual somatic growth, $s_i(x, t)$ is the weight-specific assimilation rate of consumed biomass, $u_i(x, t)$ is the density of individuals, and x is log body weight [28]. To convert this into an equation in terms of weight, we multiply somatic growth (Eq 42, Section 3.4) by the abundance density size spectrum and weight such that

$$P_i(w, t) = g_i(w, t)N_i(w, t)w. \quad (37)$$

Therefore, the fishing mortality when balanced harvesting is being implemented is

$$\mu_{BH,i}(w, t) = \begin{cases} cP_i(w, t) & \text{if } w \geq w_{\min} \\ 0 & \text{otherwise} \end{cases} \quad (38)$$

where c is a scaling constant and w_{\min} is the weight at which the selectivity function operates. Therefore the selectivity of balanced harvesting is more complex in comparison to knife-edge selectivity in Figure 5, because it varies with somatic production which is dependent on both weight and time. Equation 38 for the fishing mortality of balanced harvesting, has dimensions such that

$$[\mu_{BH,i}] = [c][P_i] \iff \frac{1}{\text{time}} = [c] \frac{\text{mass}^2}{\text{time}}. \quad (39)$$

This implies that the dimensions for c are $[c] = \frac{1}{\text{mass}^2}$.

3.4 Reproduction & Somatic Growth

In Section 3.3.1, we defined the rate of consumption (Equation 26) and now we will define the rate of assimilated consumption E_a . Assimilation is the absorption and digestion of food or nutrients by the body or any biological system [29]. The consumed food is assimilated with an efficiency coefficient α , which is used to provide energy for two processes, standard metabolism and movement. The former is at a rate kw^p and the latter at a rate kw . However, there is also the case of when the consumed food does not provide the necessary

energy for metabolism and movement, therefore we write the assimilated consumption rate as [29]

$$E_a(w) = \max(0, \alpha f(w) h w^n - k w^p - k w). \quad (40)$$

The proportion of E_a which contributes to the energy required for reproduction is given by the function $\psi(w)$, which varies between 0 and 1 [8]

$$\psi(w) = \left[1 + \left(\frac{w}{w_{\text{mat}}} \right)^{-10} \right]^{-1} \left(\frac{w}{W_\infty} \right)^{1-n}, \quad (41)$$

where w_{mat} is the size at maturity and W_∞ is the asymptotic size. Hence, somatic growth is given by [8]

$$g(w) = E_a(w)(1 - \psi(w)). \quad (42)$$

If the feeding level is set to be constant $f(w) = f_0$, then the somatic growth function approximates a von Bertalanffy growth curve [30]. However when applying empirical data to set up a model, the growth curves will be dependent on feeding levels.

Finally, we can define the reproduction rate as the production rate of eggs R , which is found by integrating over the abundance density spectrum multiplied by the assimilated consumption rate and $\phi(w)$:

$$R = \frac{\epsilon_{\text{egg}}}{2w_0} \int_0^\infty N(w) E_a(w) \phi(w) dw. \quad (43)$$

We divide the integral by 2 to account for the fact that only females reproduce, and also divide by the egg weight w_0 because that will convert the energy into the actual number of eggs. The egg production rate has a reproductive efficiency ϵ_{egg} , which was estimated by Gunderson (1997) to be $\epsilon_{\text{egg}} \approx 0.22$ [31].

3.5 Steady State Solution of the McKendrick-von-Foerster Equation

The steady state of the MvF equation is of particular interest because that is where the effects of the death rate and the changes in the growth rate exactly balance in such a way that the size spectrum stays constant over time. Steady states are an essential aspect for our size spectrum models, because setting up a model requires initialising and describing a steady state that is in agreement with current observations to calibrate our model. Then we can choose additional parameters that determine the dynamics away from the steady state [8]. We can analytically solve the MvF equation at the population level. We can set $\frac{\partial N(w)}{\partial t}$ in Equation 7 to zero because at the steady state the size spectrum is constant, and reduce the PDE to an ordinary differential equation (ODE):

$$\frac{dg(w)N(w)}{dw} = -\mu(w)N(w). \quad (44)$$

We want to rewrite this in a form where it can be integrated. To do this, note that [14]

$$\frac{d \ln(g(w)N(w))}{dw} = \frac{1}{g(w)N(w)} \frac{dg(w)N(w)}{dw}, \quad (45)$$

where we are using an example of the chain rule

$$\frac{d \ln(f(x))}{dx} = \frac{1}{f(x)} \frac{df(x)}{dx}.$$

Then we can rearrange Equation 45 for $\frac{dg(w)N(w)}{dw}$, and substitute this into Equation 44 to obtain

$$\begin{aligned} g(w)N(w) \frac{d \ln(g(w)N(w))}{dw} &= -\mu(w)N(w) \\ \iff \frac{d \ln(g(w)N(w))}{dw} &= \frac{-\mu(w)}{g(w)}. \end{aligned} \quad (46)$$

Now we can integrate both sides with respect to w :

$$\begin{aligned} \left[\ln(g(w)N(w)) \right]_{w_0}^w &= - \int_{w_0}^w \frac{\mu(w)}{g(w)} dw \\ \implies \ln\left(\frac{g(w)N(w)}{g(w_0)N(w_0)}\right) &= - \int_{w_0}^w \frac{\mu(w)}{g(w)} dw. \end{aligned} \quad (47)$$

Taking the exponential on both sides then gives us

$$\frac{g(w)N(w)}{g(w_0)N(w_0)} = \exp\left[- \int_{w_0}^w \frac{\mu(w)}{g(w)} dw\right]. \quad (48)$$

We will denote the RHS of this equation as the survival from w_0 to w , $S_{w_0 \rightarrow w}$. Additionally, note that the denominator of the LHS of this equation is the population level boundary condition (see Equation 14, Section 3.1). Therefore we can rewrite everything as

$$\frac{N(w)}{R} = \frac{1}{g(w)} S_{w_0 \rightarrow w}. \quad (49)$$

In general the survival integral is solved numerically, however there is a special case when it can be solved analytically. For this we need to use the growth as the von Bertalanffy growth model, and the mortality as the predation mortality inflicted by larger individuals, then substitute these into the survival

$$S_{w_0 \rightarrow w} = \exp\left[- \int_{w_0}^w \frac{\mu(w)}{g(w)} dw\right].$$

The von Bertalanffy growth equation is as defined in Equation 17 (Section 3.2). The mortality needed to solve the MvF equation is as defined in Equation 33 (Section 3.3.1),

which showed that predation mortality is proportional to w^{n-1} and the consumption rate $f_0 h$. However instead of carrying forward the constant coefficients f_0 , h and Φ_p , we can write the predation mortality in this simplified form [14]

$$\mu_p(w) = aAw^{n-1}. \quad (50)$$

Here, A is the same as the growth coefficient in the von Bertalanffy model and a is a dimensionless parameter that represents physiological mortality [14]. Now substituting growth and mortality into the survival we obtain

$$\begin{aligned} S_{w_0 \rightarrow w} &= \exp \left[- \int_{w_0}^w \frac{aAw^{n-1}}{Aw^n} \left[1 - \left(\frac{w}{W_\infty} \right)^{1-n} \right]^{-1} dw \right] \\ &= \exp \left[- \int_{w_0}^w aw^{-1} \left[1 - \left(\frac{w}{W_\infty} \right)^{1-n} \right]^{-1} dw \right] \\ &= \left(\frac{w}{w_0} \right)^a \left[\frac{1 - (w/W_\infty)^{1-n}}{1 - (w_0/W_\infty)^{1-n}} \right]^{\frac{a}{1-n}}. \end{aligned} \quad (51)$$

We can simplify this by noting that if $W_\infty \gg w_0$, then the denominator in the square brackets is approximately equal to 1 such that

$$S_{w_0 \rightarrow w} = \left(\frac{w}{w_0} \right)^{-a} \left[1 - \left(\frac{w}{W_\infty} \right)^{1-n} \right]^{\frac{a}{1-n}}. \quad (52)$$

Finally, by substituting the growth and survival into Equation 49 we will obtain the steady state solution of the MvF equation

$$\begin{aligned} \frac{N(w)}{R} &= \frac{w^{-n}}{A} \left[1 - \left(\frac{w}{W_\infty} \right)^{1-n} \right]^{-1} w^{-a} w_0^a \left[1 - \left(\frac{w}{W_\infty} \right)^{1-n} \right]^{\frac{a}{1-n}} \\ &= \frac{w_0^a}{A} w^{-n-a} \left[1 - \left(\frac{w}{W_\infty} \right)^{1-n} \right]^{\frac{a}{1-n}-1} \\ \implies N(w) &= R \frac{w_0^a}{A} w^{-n-a} \left[1 - \left(\frac{w}{W_\infty} \right)^{1-n} \right]^{\frac{a}{1-n}-1} \text{ for } W_\infty \gg w_0. \end{aligned} \quad (53)$$

The term in the square brackets is approximately equal to 1 for young fish, i.e. when $w \ll W_\infty$. Then as fish mature and grow, the steady state solution diverges to zero (when $a > 1 - n$). These are described as the dynamics of the abundance spectrum at the steady state (or at equilibrium). We have not addressed the stability of the steady state. However, in the work of Datta *et al.* (2011) they showed that the steady state is always unstable without diffusion, and when there is diffusion the steady state is more likely to be stable when there is a higher predator-prey mass ratio [32].

4 Implementing the Multispecies Model

4.1 Introducing `mizer`

`mizer`: Multi-Species sIZE Spectrum Modelling in R is an R package which consists of methods to set up and run multispecies, trait-based and community size spectrum ecological models, focused on the marine environment [8]. The `mizer` CRAN page can be found here: <https://cran.r-project.org/package=mizer>. We can use `mizer` to set up a multispecies model for the marine ecosystem in the Southwest of the UK, and simulate different fishing strategies to assess how that might affect the sustainability of the ecosystem. The mechanisms, parameters, and sub-models which have been described in Sections 2 and 3, are the same as those which `mizer` uses and can incorporate. There are four main stages to implement a multispecies model:

1. **Initialising the model parameters.** This involves utilising empirical data to set up three different parameter data frames: species parameters such as asymptotic weight, gear parameters such as knife-edge size, and a predator-prey interaction matrix.
2. **Setting to steady state.** This involves running the dynamics whilst keeping the reproduction and other components constant for each species, until the size spectra no longer changes (or there are only insignificant changes) [33]. Then the reproductive efficiencies are set to values that give the level of reproduction observed in that steady state.
3. **Tuning parameters.** This involves setting the scale of the system so that the total biomass in the model agrees with the total observed biomass, scaling individual size spectra for each species so that the model biomasses will match the observed biomasses, and adjusting parameters relating to growth so that the model growth curves match the von Bertalanffy growth curves [34].
4. **Exploring the results.** The results can be explored and presented using a variety of plots and summaries.

The necessary parameters to set up an initial multispecies model are described in Table 1:

Parameter	<code>mizer</code> name	Description
species	species	Species name
W_∞	w_inf	Asymptotic weight
K	k_vb	von Bertalanffy growth constant (Eq. 19)
w_{mat}	w_mat	Maturity size/mass
observed biomass	biomass_observed	Observed biomass density (kg/km^2)
μ_f	z_0	Fishing (external) mortality rate

Table 1: Table to describe the required parameters for an initial multispecies size spectrum model which includes the parameter names, the names `mizer` is programmed to call the parameters, and their descriptions.

One can then expand the model to also include predation parameters, gear parameters and species' interactions. Then, the idea behind tuning the parameters to steady state is not necessarily to re-tune the reproductive efficiency to give realistic values, but rather to adjust the other parameters in the system until the system arrives at a steady state with sensible reproductive efficiency values [33]. Behind the scenes within `mizer`, when attempting to converge to a steady state, it is finding a numerical solution of the survival as described in Equation 49 (Section 3.5).

4.2 Multispecies Model Data

The majority of the parameters outlined in Table 1 were extracted from data provided by Cefas. Therefore, in this section we will describe this Cefas data and how it correlates to the `mizer` model, discuss the data sources that were used to expand the model, and highlight the pre-processing steps and assumptions made to overcome issues related to data analysis. There were two large datasets provided by Cefas; landings data for the Celtic Sea, and survey data corresponding to the Southwest region of the UK (both of which are only accessible through a password protected sharepoint). Landings data captures fishing activity by individual vessels by trip, and for each day within a trip. This includes information of the catch by species, details on the fishing gear used and the area where the fish were caught [35]. Area is divided into statistical rectangles as defined by the International Council for the Exploration of the Sea (ICES). ICES rectangles are used to grid data onto maps to allow for simplified analysis and visualisation. Survey data is collected from four annual fish stock surveys in the UK carried out by Cefas, which details the spatial distribution and relative abundance for different species of fish [36]. It is also categorised into ICES rectangles.

The landings data used consists of over 91000 observations spanning the years 2003 to 2016, between the longitude and latitude coordinates of $1.5 - 9.5^{\circ}\text{W}$ and $48.2 - 51.8^{\circ}\text{N}$ (in the Celtic Sea). Some of the variables included in the dataset are: the average length at maturity, average asymptotic length, average asymptotic weight, and the von Bertalanffy growth constant, all of which are available for the species of interest listed in Section 1.2. The length at maturity can be converted to size later in R, and these four parameters can be directly extracted into a compiled parameter list (Appendix A).

The survey data used consists of over 40000 observations spanning the years 1998 to 2020, between the same longitude and latitude coordinates as the landings data. This dataset included a biomass density (observed biomass) variable, however each species has a different observed biomass for different haul IDs and date of catch. This means that the biomass needs to be averaged across the years; details on this can be found in the next section (Section 4.2.1). The average observed biomass for each of our species of interest can then be inputted into our compiled parameter list (Appendix A).

Technically we have now extracted all of the required parameters in Table 1 except from the fishing mortality rate. Utilising Cefas' Data Hub, I sourced a UK fish stock data

assessment relating to the years 1905 to 2020 [37], which can be accessed here <https://doi.org/10.14466/CefasDataHub.120>. The dataset includes fishing pressure for each stock each year. The assessment was split into stock assessment graphs for each species and in different regions of the UK. Therefore, the fishing (external) mortality rate parameters in the compiled list are extracted directly from searching through this stock assessment for our species of interest and in the region of the Celtic Sea. Now we have all the necessary parameters to implement an initial multispecies model in `mizer`.

To expand the model, we can think about spatial structure in terms of predator-prey interactions, because by default `mizer` will only set an interaction matrix of 1s, which assumes homogeneous mixing. We will extract the relevant entries (the species that are the same) from the interaction matrix for species in the Celtic Sea, labelled Table S2 in the supplementary material of Spence's 2021 paper [38]. The interaction matrix we input into the `mizer` model can be found in Appendix B. Furthermore, the model can be expanded by including the two parameters of the log-normal predation kernel for each species: the preferred predator-prey mass ratio β , and the width of the log-normal kernel σ . (Both of which are discussed in Section 3.3.1). By default `mizer` will use $\beta = 30$ and $\sigma = 2$. The parameter values are sourced from Table S3 in the supplementary material of Spence's paper [38], thus the values for our species of interest we will input into the model are as follows:

Species	beta	sigma
European Hake	11	1.1
Whiting	22	1.5
Haddock	558	2.1
Atlantic Cod	66	1.3
Saithe(=Pollock)	30	2
Ling	30	2
Anglerfish	16	1.2
Megrim	85	1.4
Common Sole	381	1.9
European Plaice	113	2

Table 2: Table which lists the predation parameters that describe the log-normal predation kernel for our species of interest.

4.2.1 Data Pre-Processing & Data Assumptions

Firstly, it is important to discuss how comparable the survey and landings dataset are with each other because we are drawing up a compiled list of parameters from both. In the landings dataset two species were listed as 'Anglerfishes nei' and 'Megrimis nei', with missing entries for their genus and taxonomic species name. The word 'nei' is an abbreviation of 'not enough information', and in fisheries science nei is often used to denote new or uncertain

species; it is most likely that the specific species of anglerfish and megrim were unknown. However in the survey dataset, specific species for these two types of fish were listed as *Lophius piscatorius* (anglerfish) and *Lepidorhombus whiffiagonis* (megrim). Therefore, for comparability we assume that the species of anglerfish and megrim listed in the landings data are the same as those listed in the survey data.

The R code used to extract the observed biomass parameters from the survey data can be found in Appendix C. To calculate the average observed biomass for each species we need to subset the survey dataset by our species of interest, making sure to add the taxonomic names for specific species of anglerfish and megrim too, and by fish caught with beam trawls. Next we want to group the data by haul, year and taxonomic name and sum the biomass density in each of these groups. Then, take the average biomass over time by grouping the data by taxa and calculating the mean. However, when plotting the time series of biomass density (following these same steps except grouping by taxa and year before calculating the mean), we see that the arithmetic mean we have used is being dominated by extreme outliers (Appendix C.1). Instead, we will use the geometric mean which is defined as:

$$\left(\prod_{i=1}^n x_i \right)^{\frac{1}{n}}.$$

This is incorporated into the R code in Appendix C in log form i.e.

$$\exp \left[\sum_{i=1}^n \frac{\ln(x_i)}{n} \right].$$

We can show that these two definitions are equivalent:

$$\begin{aligned} \exp \left[\sum_{i=1}^n \frac{\ln(x_i)}{n} \right] &= \exp \left[\frac{\ln(x_1)}{n} \right] \dots \exp \left[\frac{\ln(x_n)}{n} \right] \\ &= \exp[(\ln(x_1))^{\frac{1}{n}}] \dots \exp[(\ln(x_n))^{\frac{1}{n}}] \\ &= x_1^{\frac{1}{n}} \dots x_n^{\frac{1}{n}} \\ &= \left(\prod_{i=1}^n x_i \right)^{\frac{1}{n}}. \end{aligned}$$

The time series plots of the biomass density using the geometric mean has improved (reduced) the variation year on year of the observed biomass as shown in Appendix C.2. The observed biomass parameters we will use are therefore those obtained by using the geometric mean, and these are recorded in our compiled parameter list (Appendix A). One can compare the difference of these to the observed biomass parameters obtained by using the arithmetic mean in Appendix C.3.

The parameter data frame we have not yet considered are the gear parameters. `mizer` chooses knife-edge selectivity by default as the fishing gear for all species, which we shall

not change. However, we will assume that the knife-edge size is equivalent to the minimum landing size for each species as set by government regulations [39]. The source for this information can be found here <https://www.gov.uk/government/publications/minimum-conservation-reference-sizes-mcrs>, and have been added to our compiled parameter list. Additionally, we will assume that catchability is equivalent to fishing pressure/external mortality as detailed in our parameter list.

Other data and parameter assumptions are discussed below:

- To convert L_{mat} to W_{mat} we use $W_{\text{mat}} = aL_{\text{mat}}^b$. Therefore we require the values for the allometric parameters a and b , which were not included in the landings dataset. We consequently assumed that a and b were equal to an average of allometric parameters sourced from Irish sea data in Spence's 2021 paper [40], ($a = 0.006$, $b = 3$).
- We have assumed that fishing pressure is the same as fishing mortality because ICES defined fishing pressure as the change in stock size over time [37]. (We sourced the fishing mortality from an ICES stock assessment).
- Spence's interaction matrix [38] did not contain information on ling or saithe, therefore we assume they interact with all species with probability 0.7. This is an approximate average after analysing other species interactions in the Celtic Sea. Spence also considered the interactions of monkfish which are members of the genus lophus, which belongs to the lophiidae family i.e. anglerfishes. Therefore, we assume that species interactions for anglerfish were equivalent to those for monkfish as detailed by Spence.
- There is no minimum landing size for anglerfish, therefore we will assume that the knife-edge size for anglerfish is equivalent to its length at maturity (approximately 29.6cm).

5 Results

Primarily, we will calibrate a multispecies size spectrum model to the current Southwestern marine ecosystem with a constant fishing effort at minimum landing size. This will be achieved by utilising our compiled parameter list, including predation parameters and interaction matrix. We assume that the initial fishing effort is 10. Upon running the dynamics to steady state, convergence was achieved in 48 years. Figure 6 plots the resulting size spectra, and comparing the shape of the total species curve (black) to the shapes of the size spectra in Figure 4, we see they are very similar. However, note that the size spectra curves for each species rapidly decrease to zero when fish become very large in size.

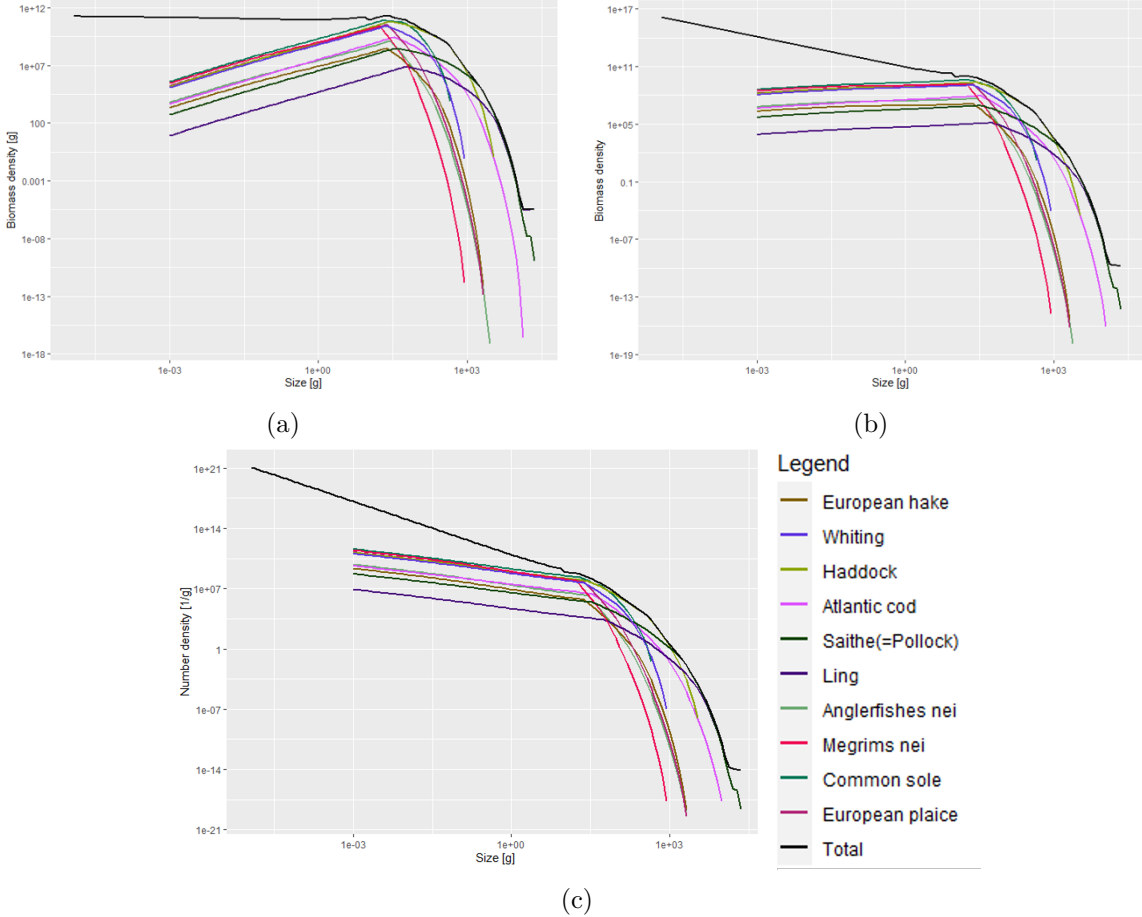
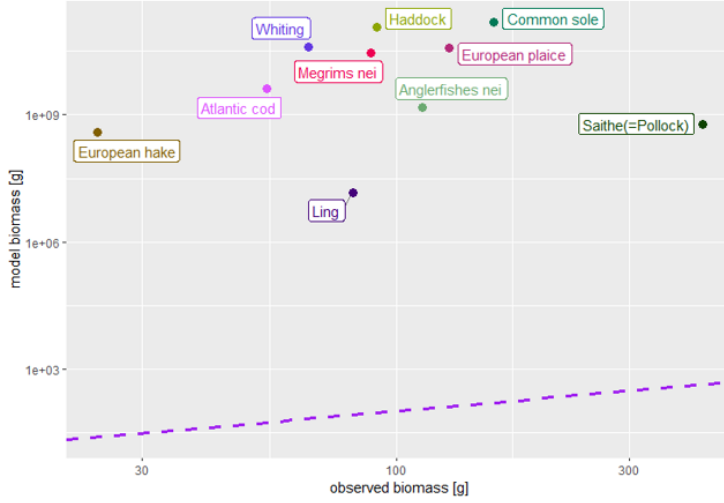
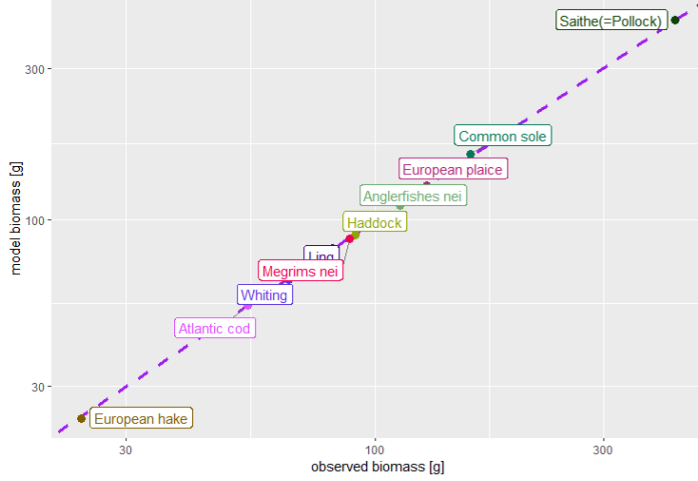


Figure 6: Three size spectrum plots for the Southwest marine ecosystem with constant fishing level at minimum landing size before calibration: the Sheldon spectrum (a), the biomass spectrum (b), and the abundance spectrum (c).

We need to compare these biomasses with our observed biomasses. Figure 7a plots the biomass of each species in our model against the observed biomasses that are listed in our original compiled parameters (from empirical data). We can see that they definitely do not agree, because `mizer` does not know how big our model ecosystem is, so the scale is arbitrary [33]. Therefore, we need to tune our model by calibrating and matching our model biomasses to the observed biomasses. This can be achieved using a shiny gadget that is within `mizer`, (see Appendix D.1 for an example of the gadget interface). Calibrating the biomasses means we are choosing the scale of the system so that the total biomass in the model agrees with the total observed biomass, and matching the biomasses means we are moving the spectra for individual species so that the total spectrum roughly follows a power law [33]. Figure 7b shows the resulting plot of the model biomasses against the observed biomasses after tuning.



(a) Before calibrating and matching



(b) After calibrating and matching

Figure 7: Plot of the observed biomasses obtained from Cefas data, against the model biomasses for each species.

Tuning the growth curves was also required to calibrate our model to the current Southwestern marine ecosystem. This could be achieved via the shiny gadget too, by increasing the search volume γ for each species such that the model growth curves approximate the von Bertalanffy growth curves (as determined by our parameters extracted from Cefas data). The before and after growth parameter tuning plots for each species can be found in Appendix D.2. After tuning any parameters, the dynamics need to be run back to steady state. We now have an updated list of parameters that represent the current ecosystem, which we can project forward in time where the initial conditions

are set to the steady state. The saved parameter file along with other R files and datasets can be found in the GitHub repository <https://github.com/krl516/MMathProject>.

We project a size spectrum model simulation forward in time 75 years with constant fishing effort of 10 at minimum landing size for each species. Figure 8 shows the biomass spectra and the biomass of each species plotted against time, after running the simulation on our calibrated model. The shape of the plot in Figure 8a is similar to that in Figure 6b, however note the change in scale. The biomasses of each species in Figure 8b remain approximately constant over time, which we would expect to see because the initial conditions for the simulation were set to steady state and the fishing effort does not vary with time. We can compare this system against different fishing scenarios: a system with no fishing, and a system that implements balanced harvesting.

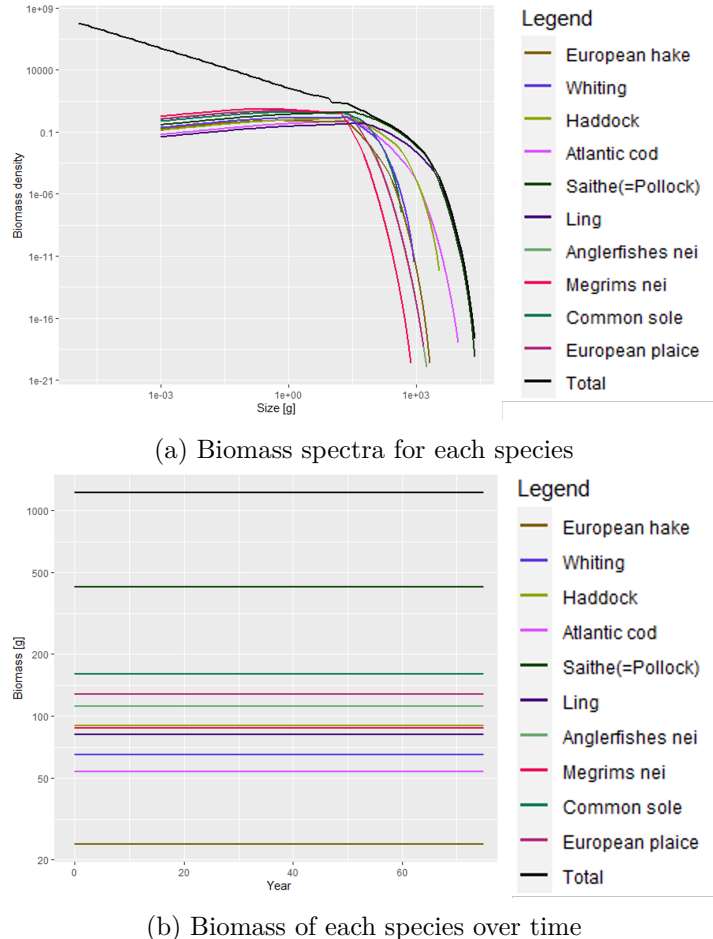
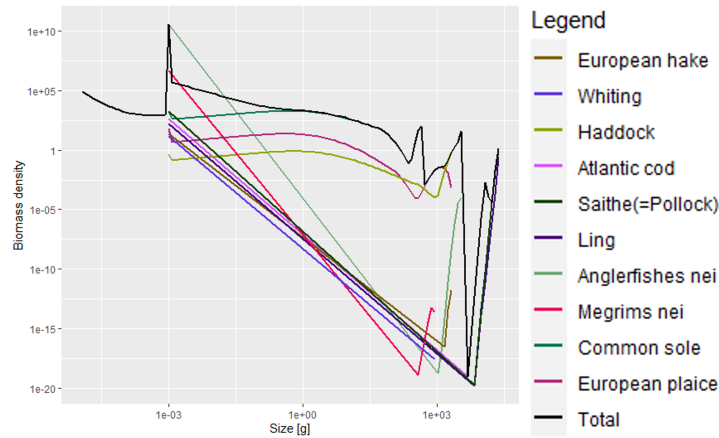
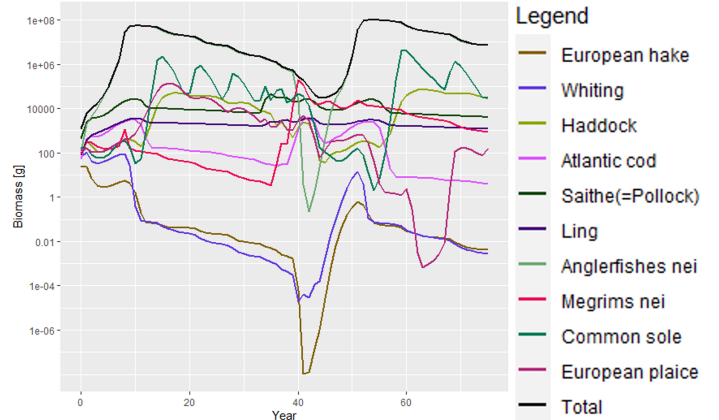


Figure 8: Plots obtained after running a size spectrum model simulation forward in time for 75 years, with constant fishing effort of 10 at minimum landing size for each model species, using parameters calibrated to the current ecosystem in the Southwest.

Firstly, to simulate a system without fishing we can set the fishing effort to zero, then re-run the system to steady state. The resulting biomass spectra and biomasses of each species over time are shown in Figure 9. By comparison to a system with constant fishing, in Figure 9b we see that the biomasses for all the species now vary over time. Additionally in contrast to the system with fishing, the total biomass spectrum in Figure 9a has a couple of peaks and does not directly decrease to zero for species larger than 1000g. Instead, for the majority of species the biomass densities gradually decrease as fish grow, however rise again for the largest fish. The average slope of the total biomass spectrum for species between 0.01g and 1000g is -0.8117456 for the unfished system and -0.4367606 for the fished system.



(a) Biomass spectra for each species



(b) Biomass of each species over time

Figure 9: Plots obtained after running a size spectrum model simulation forward in time for 75 years, with fishing effort set to zero for each model species, using parameters calibrated to the current ecosystem in the Southwest.

Now we can compare the total abundances of all species at size when the system is fished and unfished. Figure 10a shows that there is a clear initial impact of fishing on species approximately larger than 500g, because the fishing pressure lowers their abundance. This then relieves the predation pressure on their smaller prey, leading to an increase in their abundance. This in turn increases the predation mortality on their smaller prey, which reduces their abundance and so on until the abundance decreases to zero. This impact can also be seen by looking at Figure 10b, which plots the predation mortality of cod by size in both fishing scenarios. (One species was chosen for readability). The predation mortality is far greater in the unfished system than in the fished system.

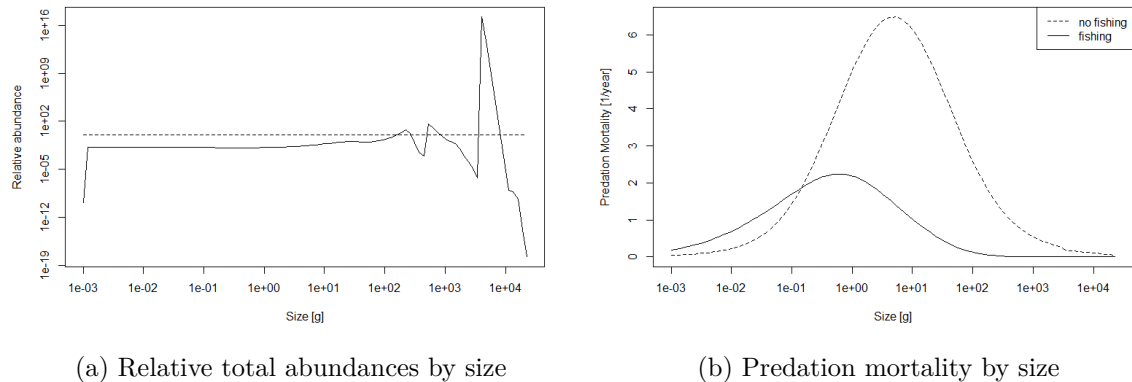


Figure 10: A comparison of fish and unfished systems: relative total abundance obtained by dividing the total abundance of the fished system by the total abundance of the unfished system (a), predation mortality for cod by size in the fished and unfished systems (b).

Another fishing scenario we can simulate within our calibrated model of the current Southwestern ecosystem, is that of balanced harvesting (BH). This is achieved by changing the gear selectivity to be equivalent to somatic production, $P_i(w, t)$ in Equation 38. Then setting catchability to equal 1 for all species, such that fishing mortality depends on production rather than having different catchability values for different species. Finally assume that the fishing effort is equivalent to the scaling constant c in Equation 38. After this, the system is run to steady state and the observed biomasses and growth curves are tuned in the same way as the constant fishing at min landing size model. After running to steady state, the initial abundances for each species in this system are approximately 10,000 times greater than in the constant fishing at min landing size system. Therefore, we set the initial fishing effort to 100,000 to allow for a more reasonable comparison between the two fishing systems. Using this BH model that is now calibrated to the current ecosystem, we project a simulation forward in time 75 years as before. The results from which are shown in Figure 11. The overall shape of the total biomass spectrum in Figure 11a is fairly similar to that in the constant fishing system (Figure 8a), with the general trend being that the biomass density of fish decreases with size. However, there is

more variation in the BH scenario, rather than a smooth decrease down to zero. The average slope of the total biomass spectrum for species between 0.01g and 1000g in the BH scenario is -1.291445 , so steeper than both of the other two systems. In Figure 11b, we see that the biomasses for the majority of species very slightly increase over time, whereas ling becomes extinct. This may be because ling are an extremely slow growing fish, therefore they are predated on and fished before high reproduction numbers can occur.

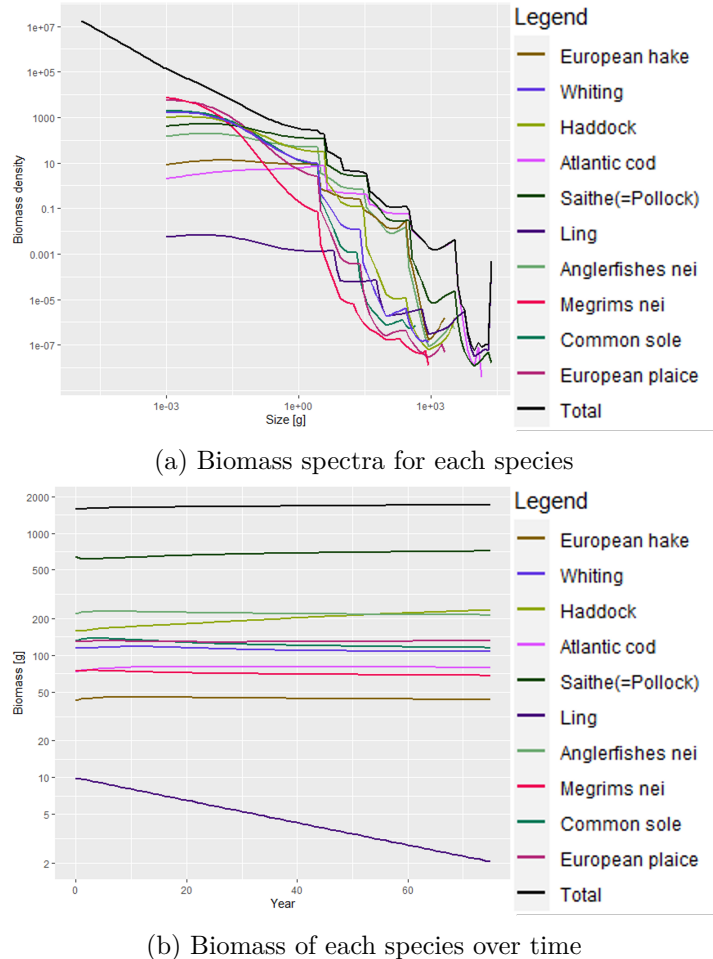


Figure 11: Plots obtained after running a size spectrum model simulation forward in time for 75 years, with balanced harvest fishing implemented, using parameters calibrated to the current ecosystem in the Southwest. The BH simulation involves increasing the fishing effort in response to larger initial abundances than the fishing at min landing size simulation.

To compare the two fishing systems, we will observe the total yield [1/year] and total biomass [kg/km^2] of each fishing method over time. In Figure 12a, the total yield obtained from the constant fishing system remains approximately constant at around 2908, and the

yield for the BH system increases by around 46% over the 75 years. The BH yield is far greater than the constant fishing yield, because when running the models to steady state the initial abundances for the BH model were greater than the abundances for the fishing at min landing size model. This is what we would expect given the higher initial abundances, however this means it is not ideal to compare the yields of the two models in their current states. In Figure 12b, the total biomass for the constant fishing system also remains approximately constant over time at 1226, and the total biomass for the BH system increases by around 7% over the 75 years.

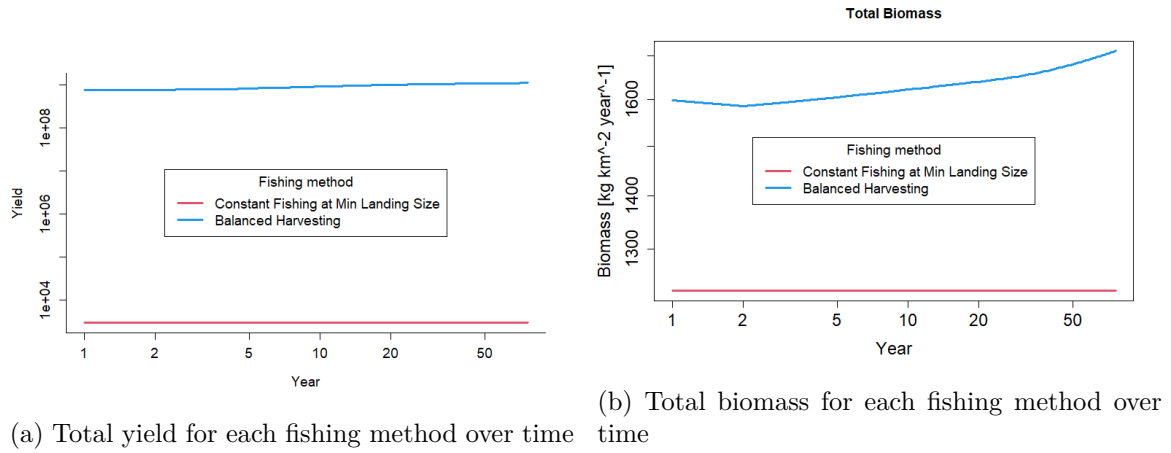


Figure 12: A comparison of constant fishing at min landing size and balanced harvesting: total yield (a), total biomass (b). The BH simulation involves increasing the fishing effort in response to larger initial abundances than the fishing at min landing size simulation.

An alternative method of handling the differences in initial abundances, is to utilise the steady state conditions of the constant fishing at min landing size model as our initial simulation conditions for balanced harvesting. In this way, we are solely changing the fishing method without re-running to steady state, therefore the initial abundances for our balanced harvesting model will remain unchanged from the original constant fishing model. We shall call this new version Balanced Harvesting II (BH2), where the fishing effort (i.e. the scaling constant c) is equal to 0.1, because that means the fishing mortality for both the fishing at min landing size and BH2 models are similar and comparable. The corresponding biomass spectra and biomass of each species over time after projecting this model forward for 75 years are shown in Figures 13a and 13b. The average slope of the total biomass spectrum for species between 0.01g and 1000g in the BH2 scenario is -1.039897 , so steeper than the constant fishing system but not as steep as the BH model. Figure 13b shows that the biomass for all species converge after approximately 10 years. However, there is an initial increase in biomass across all species before convergence. This is because initially there are mostly small species in the model, meaning most individuals have low productivity.

Therefore, these individuals will not be fished, and hence they have the opportunity to grow.

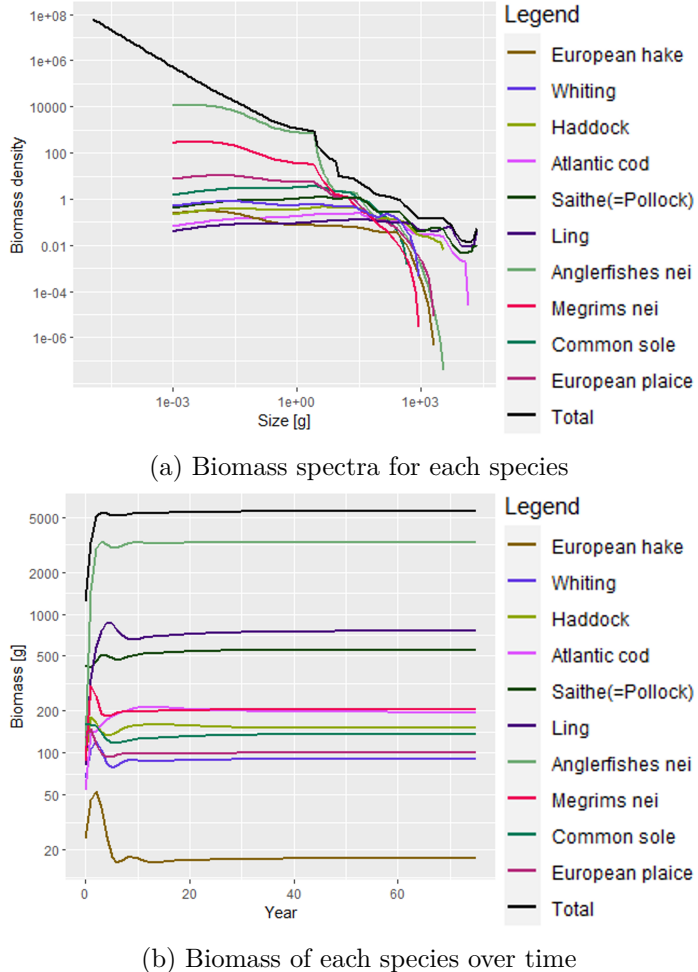


Figure 13: Plots obtained after running a size spectrum model simulation forward in time for 75 years, with balanced harvest fishing implemented, using parameters calibrated to the current ecosystem in the Southwest. The BH2 simulation involves using the same initial abundances as the min landing size simulation, without re-running to steady state.

Figure 14a plots a comparison of the total yields for our BH2 and constant fishing simulations. Now we observe that the yield of BH2 gradually increases, until it plateaus after approximately 10 years. This results in a similar curve shape as those for the biomasses over time in Figure 13b. The justification behind the curve shapes in Figure 13b, explains why the yield gradually increases, because it is representative of the notion that as fish grow, their productivity increases. The average total yield over time is greater for the BH2 model than the fishing at min landing size model, converging at

approximately 11361. In Figure 14b, the total biomass for the BH2 model increases and converges at approximately 5500. For similar reasons behind the shape of the total yield curve over time, the total biomass curve over time for BH2 increases initially because the smaller individuals are allowed to grow due to their low productivity, before then gradually being fished as they increase in size.

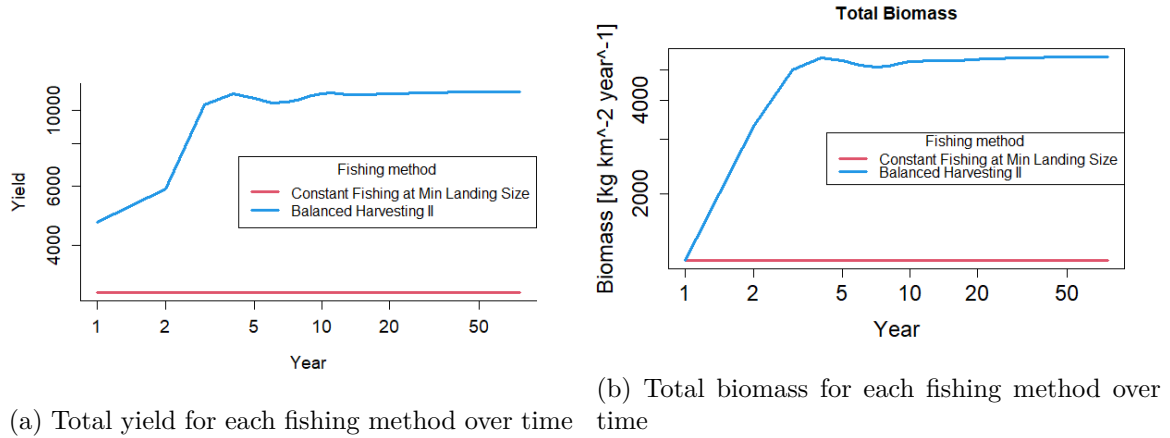
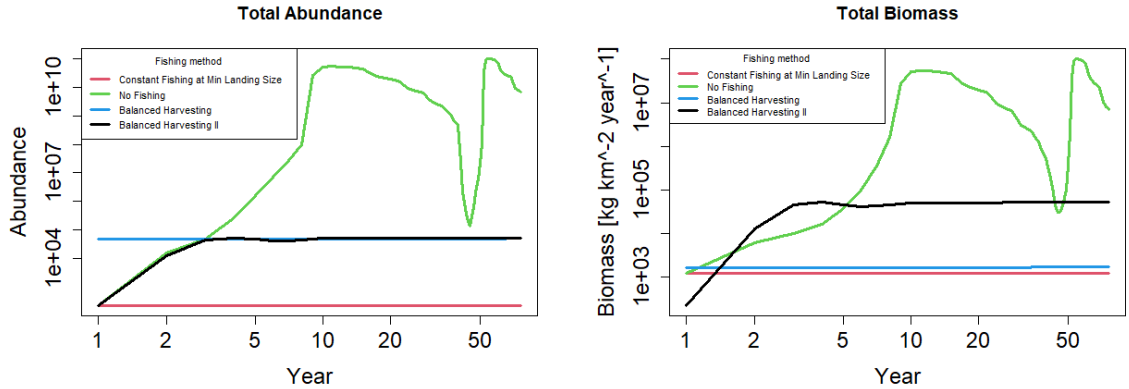


Figure 14: A comparison of constant fishing at min landing size and balanced harvesting: total yield (a), total biomass (b). The BH2 simulation involves using the same initial abundances as the min landing size simulation, without re-running to steady state.

Finally, in Figure 15 we can compare all fishing methods by observing the total abundances and total biomasses over time. It is clear that in a system where there is no fishing, the abundance of species has the chance to fluctuate over time compared to a system where there is fishing, because predation is the primary cause of death rather than fishing. In Figure 15a, the total abundance in the constant fishing system is approximately constant at 219, the total abundance in the BH system slightly increases over time and has an average of 47745, and the total abundance in the BH2 system converges at approximately 49755. On the other hand, the total abundance of the system without any fishing varies from 219 to over 100 billion. Figure 15b compares the total biomasses over time for each fishing method. We can observe from the shape of the total abundance and total biomass curves of the no fishing system, the proportionate relationship between abundance and biomass (discussed in Section 2.1).



(a) Total abundance for each fishing method over time (b) Total biomass for each fishing method over time

Figure 15: A comparison of constant fishing at min landing size, no fishing and two versions of balanced harvesting: total abundance (a), total biomass (b).

6 Discussion

We have been able to parameterise and calibrate a multispecies size spectrum model to the current marine ecosystem in the Southwest of the UK. The similarity in our size spectra obtained when implementing a constant fishing effort at the minimum landing size for each species (Fig.6), to the general shape of the size spectra accepted within ecological literature (Fig.4) is important. This is because the similarity implies that in this system, biomass is invariant over logarithmically equal size intervals (Sheldon spectrum), and abundance declines as body size increases. These relationships agree with the idea that larger prey eat smaller predators, and individuals are eaten or fished before they become very large. This trend follows through to the tuned model simulations (Fig.8a) too, where it is also true that biomass is invariant over time. Hence, suggesting that constant fishing effort across all species would not disrupt the balance of an ecosystem.

There is a stark difference between a system where there is fishing and one where there is not. When there is not any fishing being implemented in the model, we see far more variation in the species biomass (Fig.9b). This is due to predator-prey cycles, which did not have an effect when we had constant fishing effort i.e. predator abundance was always limited through fishing. Since predation mortality is the main cause of death, certain predators will become over-abundant, then decrease again where there is not enough food to sustain them, and so on. This notion is evident when comparing the predation mortality in both systems (Fig.10b), as we see much greater levels of predation in the unfished system. Hence why we don't see fluctuation in the fished system. This can also be observed in the shape of the size spectra for the unfished system (Fig.9a). There are multiple peaks along the size

spectra which correlate to this predator-prey cycle, with the main difference being that the spectra rise again for the largest fish because large fish are not being caught and will not be predated on either by smaller fish. Whereas in the fished system, eventually all fish are caught because the size spectra decrease rapidly to zero for large sizes.

It is difficult to compare sustainability between constant fishing and balanced harvesting. Petchey & Belgrano (2010) found that observed size spectra typically become steeper (more negative) following exploitation [41]. The slope of the total biomass size spectrum in the balanced harvesting scenarios (Fig.11a, 13a), where individuals are exploited in proportion to their productivity, produces the steepest curves out of the different fishing regimes. This implies balanced harvesting has the greatest exploitation, which further corresponds to it having the highest yield (Fig.12a, Fig.14a). However, there is also little change in the biomass composition of the ecosystem (Fig.11b, 13b) in relation to the system with constant fishing effort, such that the biomasses still converge. There are vast differences however between the biomass structure as a consequence of balanced harvesting, and the system without fishing. This is because fishing reduces competition and predation within the ecosystem. These results align with other recent modelling studies, which predict that balanced harvesting generates higher yields with small change in relative biomass composition compared to traditional fishing methods [28, 42]. Despite there being small change to the biomass structure in general, it is interesting to note that for both the BH2 and constant fishing simulations, European hake was the most vulnerable species such that it had the lowest biomass (Fig.8b, Fig.13b). This suggests it is advisable that hake should not be greatly fished. Finally, comparing the abundance of all regimes highlights the importance fishing has on maintaining biomass structure (Fig.15a). For example, if a system is left unfished the abundance of fish increases to unsustainable levels that would impact other ecosystems.

It is important to critique this model and discuss ways in which it can be furthered. For example, when implementing most fishing regimes we ran the dynamics to steady state and used those conditions as the initial conditions for our simulations. This meant that the initial abundances for each species in the model were different for each of these fishing methods, which makes it harder to compare the results even when re-scaling the fishing effort in an attempt to counterbalance the abundance differences. Although we ran the BH2 model which did not involve re-running the dynamics to steady state, in future models it would be useful to explore exactly how converging to steady state affects the initial abundances. Furthermore, it is vital that we explore how we can calculate the scaling constant c for balanced harvesting simulations to ensure that the simulations results for different fishing methods are comparable. Additionally, Spence's Celtic Sea data that was used to parameterise an interaction matrix and predation [38], did not have data for ling, and this was the only species in the initial BH model (and across all models) which faced extinction. Therefore, the results we saw for ling may be a direct consequence of the assumptions we made about its interaction with the other species. As a result, it is important we try to source this information about ling in the Celtic Sea through the Cefas

data hub in future variations of our model.

In terms of expanding the model, there are capabilities to simulate a wider range of fishing scenarios such as seasonal fishing and real-life quotas. To parameterise this, we would require information on the types of fishing gear used to target particular species and their fishing intensities throughout the year. In this way, we can calibrate the model to the current fishing strategies used in the Southwest of the UK to gain a better understanding of exploitation and biomass structure. Furthermore, there are numerous other parameters that `mizer` has the capability of involving in size spectrum models, many of which are discussed throughout Section 3. With regard to species parameters, these include egg size, feeding level and assimilation efficiency. A comprehensive list of potential model parameters within `mizer` can be found here https://sizespectrum.org/mizer/articles/images/cheat_sheet.pdf.

7 Conclusion

We have established that multispecies size spectrum modelling is an effective method for understanding the abundance and biomass structures of a marine ecosystem, in terms of different species size groups or trophic levels. This is because they provide indicators of ecosystem status (i.e. over-exploited, sustainable etc), and can be used to calculate reference states in fisheries [41]. We have successfully parameterised the first initial multispecies model for the marine ecosystem in the Southwest of the UK using a variety of data sources, including landings and survey data provided by Cefas. Then calibrated the model to the current ecosystem by running the dynamics to steady state, re-tuning the parameters so that the model biomasses and growth curves matched the observed biomasses and von Bertalanffy growth curves, and so on. Using the steady state conditions as the initial conditions for simulations, we projected the model dynamics forward in time for 75 years for three different fishing regimes. Therefore, we were able to achieve our primary aim (Section 1.2).

We explored the biomass spectra and how biomass varied over time when: there is constant fishing at minimum landing size, there is no fishing, and balanced harvesting is implemented. By comparing these results as well as the total abundance, total biomass, and total yield for each fishing method over time, we found that the balanced harvesting scenarios produced the steepest total biomass spectrum curves. This implies that this method is the most exploitative in terms of producing the highest total yield. However, the biomass structure under the balanced harvesting scenarios remained generally constant over time, and the biomass densities gradually decreased with size. Similar observations were also found under the constant fishing effort scenario, suggesting that both methods could be sustainable, but balanced harvesting is preferable with it providing the higher yield. However, implementing either of these methods in real life is difficult because fishing has other dependencies which we have not considered, such as consumer demand for specific species. On another note, we were able to highlight the stark differences between a system that is fished and one that is not. This is because we saw large variation in biomass over time and a rise in

biomass density for the largest sized fish, for the unfished system. We established that this would be due to the impacts of predator-prey cycles, which were ineffective in the fished systems. Therefore, we have learned how the Southwestern marine ecosystem functions under different fishing regimes, hence achieving our secondary aim (Section 1.2).

In regards to the wider Pyramids of Life project, our multispecies model and R code framework can be used as a base structure, which can then be expanded on by adding various other model parameters that Cefas has the data for. In this way it is possible for the Pyramids of Life project to achieve one of their deliverables; identifying changes in fisheries management to maintain a sustainable ecosystem. Additionally, our results can be utilised as preliminary results for the wider project, such that they motivate which plots and measurements provide what type of insight. Finally, this report has highlighted the need to understand exactly how initial abundances are affected by converging the dynamics to steady state. It has also highlighted that we need to find methods to improve implementing and comparing balanced harvesting simulations to other scenarios, in terms of handling differences in initial abundances and calculating our scaling constant c .

References

- [1] Datta S., Delius G. W., and Law R. “A jump-growth model for predator–prey dynamics: derivation and application to marine ecosystems”. In: *Bulletin of Mathematical Biology* 72.6 (2010), pp. 1361–1382.
- [2] Jennings S. et al. “Weak cross-species relationships between body size and trophic level belie powerful size-based trophic structuring in fish communities”. In: *Journal of Animal Ecology* (2001), pp. 934–944.
- [3] Garcia S. M. et al. “Reconsidering the consequences of selective fisheries”. In: *Science* 335.6072 (2012), pp. 1045–1047.
- [4] Kituyi M. and Thomson P. *90% of fish stocks are used up - fisheries subsidies must stop | United Nations Conference on Trade and Development*. 2018. URL: <https://unctad.org/news/90-fish-stocks-are-used-fisheries-subsidies-must-stop>. (Accessed: 21.11.2021).
- [5] Pitchford J. W. “Pyramids of Life Research Proposal. Submitted to NERC SMMR programme 2020 (funded from July 2021)”.
- [6] Food and Agriculture Organization of The United Nations (FAO). *The State of World Fisheries and Aquaculture (SOFIA)*. 2020.
- [7] Internation Council for the Exploration of the Sea (ICES). *Celtic Seas ecoregion - Fisheries overview*. Nov. 2020. URL: https://www.ices.dk/sites/pub/Publication%5C%20Reports/Advice/2020/2020/FisheriesOverviews_CelticSeas_2020.pdf.

- [8] Scott F., Blanchard J. L., and Andersen K. H. “Mizer: An R package for multispecies, trait-based and community size spectrum ecological modelling”. In: *Methods in Ecology and Evolution* 5.10 (2014), pp. 1121–1125.
- [9] Pikitch E. K. “The risks of overfishing”. In: *Science* 338.6106 (2012), pp. 474–475.
- [10] Sheldon R. W. and Parsons T. R. “A Continuous Size Spectrum for Particulate Matter in the Sea”. In: *Journal of the Fisheries Research Board of Canada* 24.5 (1967), pp. 909–915. DOI: 10.1139/f67-081.
- [11] Boudreau P. R., Dickie L. M., and Kerr S. R. “Body-size spectra of production and biomass as system-level indicators of ecological dynamics”. In: *Journal of theoretical biology* 152.3 (1991), pp. 329–339.
- [12] Kerr S. R. and Dickie L. M. *The biomass spectrum: a predator-prey theory of aquatic production*. Columbia University Press, 2001.
- [13] Andersen K. H., Jacobsen N. S., and Farnsworth K.D. “The theoretical foundations for size spectrum models of fish communities”. In: *Canadian Journal of Fisheries and Aquatic Sciences* 73.4 (2016), pp. 575–588. DOI: 10.1139/cjfas-2015-0230.
- [14] Andersen K. H. *Fish ecology, evolution, and exploitation*. Princeton University Press, 2019.
- [15] Sheldon R. W., Prakash A., and Sutcliffe Jr W. H. “The size distribution of particles in the ocean 1”. In: *Limnology and oceanography* 17.3 (1972), pp. 327–340.
- [16] Law R. et al. “Size-spectra dynamics from stochastic predation and growth of individuals”. In: *Ecology* 90.3 (2009), pp. 802–811.
- [17] Zhang L. et al. “Trait diversity promotes stability of community dynamics”. In: *Theoretical Ecology* 6.1 (2013), pp. 57–69.
- [18] Pozniak H. “Smart motorways: what are they good for? [Infrastructure-Road Networks]”. In: *Engineering & Technology* 15.7 (2020), pp. 56–59.
- [19] Brander K. “Reduced growth in Baltic Sea cod may be due to mild hypoxia”. In: *ICES Journal of Marine Science* 77.5 (2020), pp. 2003–2005.
- [20] Rochet M. J. and Benoît E. “Fishing destabilizes the biomass flow in the marine size spectrum”. In: *Proceedings of the Royal Society B: Biological Sciences* 279.1727 (2012), pp. 284–292.
- [21] McKendrick A. G. “Applications of mathematics to medical problems”. In: *Proceedings of the Edinburgh Mathematical Society* 44 (1925), pp. 98–130.
- [22] von Foerster H. “Some remarks on changing populations”. In: *The Kinetics of Cellular Proliferation*, Grune and Stratton (1959), pp. 382–407.
- [23] von Bertalanffy L. “Quantitative laws in metabolism and growth”. In: *The quarterly review of biology* 32.3 (1957), pp. 217–231.
- [24] Ursin E. *On the prey size preferences of cod and dab*. Danmarks Fiskeri-og Havundersøgelser, 1973.

- [25] Armstrong J. B. and Schindler D. E. “Excess digestive capacity in predators reflects a life of feast and famine”. In: *Nature* 476.7358 (2011), pp. 84–87.
- [26] Andersen K. H. and Beyer J. E. “Asymptotic size determines species abundance in the marine size spectrum”. In: *The American Naturalist* 168.1 (2006), pp. 54–61.
- [27] Arreguín-Sánchez F. “Catchability: a key parameter for fish stock assessment”. In: *Reviews in fish biology and fisheries* 6.2 (1996), pp. 221–242.
- [28] Law R. and Plank M. J. “Balanced harvesting could reduce fisheries-induced evolution”. In: *Fish and Fisheries* 19.6 (2018), pp. 1078–1091.
- [29] Andersen K. H., Beyer J. E., and Lundberg P. “Trophic and individual efficiencies of size-structured communities”. In: *Proceedings of the Royal Society B: Biological Sciences* 276.1654 (2009), pp. 109–114.
- [30] Hartvig M., Andersen K. H., and Beyer J. E. “Appendix A Supplementary Data: Food web framework for size-structured populations”. In: *Journal of theoretical Biology* 272.1 (2011), pp. 113–122.
- [31] Gunderson D. R. “Trade-off between reproductive effort and adult survival in oviparous and viviparous fishes”. In: *Canadian Journal of Fisheries and Aquatic Sciences* 54.5 (1997), pp. 990–998.
- [32] Datta S. et al. “A stability analysis of the power-law steady state of marine size spectra”. In: *Journal of Mathematical Biology* 63.4 (2011), pp. 779–799.
- [33] Delius G. W. *A 5-step recipe for tuning the model steady state*. mizer blog. Aug. 2021. URL: <https://blog.mizer.sizespectrum.org/posts/2021-08-20-a-5-step-recipe-for-tuning-the-model-steady-state/>.
- [34] Delius G. W. *Tuning growth curves with a shiny gadget*. mizer blog. Sept. 2021. URL: <https://blog.mizer.sizespectrum.org/posts/2021-09-07-tuning-growth-curves-with-a-shiny-gadget/>.
- [35] Marine Management Organisation. *Fishing data collection, coverage, processing and revisions*. Accessed Mar. 29, 2022 [Online]. Jan. 2021. URL: <https://www.gov.uk/guidance/fishing-activity-and-landings-data-collection-and-processing>.
- [36] Cefas. *Fisheries Surveys*. Accessed Mar. 29, 2022 [Online]. URL: <https://www.cefas.co.uk/services/surveys/fisheries/>.
- [37] Lynam C. et al. Cefas, UK. *International (ICES) and national (UK) fish stock and shellfish stock data from 2020 assessment year*. Jan. 2021. DOI: <https://doi.org/10.14466/CefasDataHub.120>.
- [38] Spence M. A. et al. “Quantifying uncertainty and dynamical changes in multi-species fishing mortality rates, catches and biomass by combining state-space and size-based multi-species models”. In: *Fish and Fisheries* 22.4 (2021), pp. 667–681.

- [39] Marine Management Organisation. *Statutory Guidance: Minimum Conservation Reference Sizes (MCRS) in UK waters*. Accessed Jan. 24, 2022 [Online]. Nov. 2018. URL: <https://www.gov.uk/government/publications/minimum-conservation-reference-sizes-mcrs/minimum-conservation-reference-sizes-mcrs-in-uk-waters>.
- [40] Spence M. A. et al. “The Use of a Length-Structured Multispecies Model Fitted Directly to Data in Near-Real Time as a Viable Tool for Advice”. In: *Frontiers in Marine Science* (2021), p. 1373.
- [41] Petchey O. L. and Belgrano A. *Body-size distributions and size-spectra: universal indicators of ecological status?* 2010.
- [42] Jacobsen N. S., Gislason H., and Andersen K. H. “The consequences of balanced harvesting of fish communities”. In: *Proceedings of the Royal Society B: Biological Sciences* 281.1775 (2014), p. 20132701.

A Compiled List of Original Model Parameters

Species of interest	Scientific name	L_mat	L_inf	W_inf	Observed Biomass (kg/km^2)	Minimum landing size (cm)	Growth coefficient K	Fishing (external) mortality rate
European hake	<i>Merluccius merluccius</i>	32.21221	80.25878	1898.6398	24.21372	27	0.140354938	0.73
Whiting	<i>Merlangius merlangus</i>	25.97623	44.63664	781.4899	65.87087	27	0.292296097	0.64
Haddock	<i>Melanogrammus aeglefinus</i>	37.04945	66.61867	3211.995	90.76385	30	0.238768679	0.55
Atlantic cod	<i>Gadus morhua</i>	48.35585	104.49061	11398.8311	54.0649	35	0.168489075	0.94
Saithe(=Pollock)	<i>Pollachius virens</i>	61.13331	115.33393	19780.9674	425.04543	35	0.135178766	0.49
Ling	<i>Molva molva</i>	78.64274	144.87776	22552.3729	81.32781	63	0.118577201	0.40
Anglerfishes nei	<i>Lophiidae (Lophius piscatorius)</i>	29.60803	67.04554	3073.1866	112.64315	none	0.110838957	1.16
Megrims nei	<i>Lepidorhombus spp (Lepidorhombus whiffagonis)</i>	19.51669	42.77967	753.3898	88.30789	20	0.154853753	1.20
Common sole	<i>Solea solea</i>	19.28694	38.32501	408.8836	158.16907	24	0.323983512	0.35
European plaice	<i>Pleuronectes platessa</i>	25.12369	52.72452	1806.81	128.18174	27	0.138225442	1.08

Figure 16: A compiled list of the parameters required to set up an initial multispecies model in `mizer`, extracted from various data sources including Cefas and ICES data.

B Species Interaction Matrix

	European Hake	Whiting	Haddock	Atlantic Cod	Saithe (=Pollock)	Ling	Anglerfish	Megrim	Common Sole	European Plaice
European Hake	1	0.782	0.889	0.731	0.7	0.7	0.797	0.826	0.305	0.486
Whiting	0.782	1	0.788	0.796	0.7	0.7	0.693	0.639	0.354	0.592
Haddock	0.889	0.788	1	0.726	0.7	0.7	0.767	0.792	0.311	0.533
Atlantic Cod	0.731	0.796	0.726	1	0.7	0.7	0.721	0.6358	0.374	0.575
Saithe (=Pollock)	0.7	0.7	0.7	0.7	1	0.7	0.7	0.7	0.7	0.7
Ling	0.7	0.7	0.7	0.7	0.7	1	0.7	0.7	0.7	0.7
Anglerfish	0.797	0.693	0.767	0.721	0.7	0.7	1	0.699	0.338	0.52
Megrim	0.826	0.639	0.792	0.638	0.7	0.7	0.699	1	0.7	0.425
Common Sole	0.305	0.354	0.311	0.374	0.7	0.7	0.338	0.242	1	0.421
European Plaice	0.486	0.592	0.533	0.575	0.7	0.7	0.52	0.425	0.421	1

Figure 17: Species interaction matrix to implement into a multispecies `mizer` model, sourced and adapted from Spence (2021) [38].

C Code to Extract the Observed Biomass

```
1 pkgs = c("tidyverse", "mapplots", "ggpubr", "RColorBrewer", "dplyr")
2 for(p in pkgs){
3   if(!require(p, character.only = TRUE)) install.packages(p)
4   library(p, character.only = TRUE)
5 }
6
7
8 load('South_west_survey_data.Rdata') #Load survey dataset
9 load('landings_data_processed.Rdata') #Loading landing dataset
10
11
12 #Choose our species of interest
13 spp_list = c('Atlantic cod', 'European plaice', 'Common sole', 'Haddock', 'Whiting',
14   ↪ 'Anglerfishes nei', 'Saithe(=Pollock)', 'Ling', 'Megrimis nei', 'European hake')
15 tax_list = unique(subset(land_df, English_name %in% spp_list)$new_taxa) %>% c('Lophius
16   ↪ piscatorius', 'Lepidorhombus whiffiagonis') #Pulls out the taxonomic names which
17   ↪ appear in both SW Survey data and Celtic sea landings data
18
19 #Average observed biomass across the years
20 survey.avg = surv_df %>%
21   filter(taxa %in% tax_list,
22     gear == 'beam') %>%
23   #Sum by haul first
24   group_by(taxa, year, HaulID) %>%
25   summarise(kgkm = sum(DensBiom_kg_Sqkm)) %>%
26   filter(!is.na(kgkm)) %>%
27   #Take mean over time
28   group_by(taxa) %>%
29   summarise(av_kgkm=mean(kgkm)) %>%
30   ungroup()
31 survey.avg
32
33 #Average biomass over years
34 survey.trends = surv_df %>%
35   filter(taxa %in% tax_list) %>%
36   #Sum by haul first
37   group_by(HaulID, year, taxa) %>%
38   summarise(kgkm = sum(DensBiom_kg_Sqkm)) %>%
39   #Take mean over time
40   group_by(taxa, year) %>%
```

```

38   summarise(av_kgkm=mean(kgkm)) %>%
39   ungroup()
40 survey.trends
41
42 #Plot average biomass time series
43 p<- ggplot(survey.trends, aes(x=year, y=av_kgkm)) +
44   geom_line(color="grey") +
45   geom_point(color="blue") +
46   facet_wrap(~taxa, scales="free") +
47   theme_minimal(base_size = 9) +
48   theme(axis.text.x = element_text(angle = 45,
49                                     hjust = 1)) +
50   labs(title = "Mean observed biomass",
51        x = "Year",
52        y = "Average biomass density (kg/km^2)")
53 p
54
55 ### USE GEOMETRIC MEAN TO MINIMISE THE DOMINANCE OF OUTLIERS FOR THE ARITHMETIC MEAN ###
56
57 #Average observed biomass across the years
58 survey.geoavg = surv_df %>%
59   filter(taxa %in% tax_list,
60         gear == 'beam') %>%
61   #Sum by haul first
62   group_by(taxa, year, HaulID) %>%
63   summarise(kgkm = sum(DensBiom_kg_Sqkm)) %>%
64   filter(!is.na(kgkm)) %>%
65   #Take mean over time
66   group_by(taxa) %>%
67   summarise(av_kgkm=exp(mean(log(kgkm)))) %>%
68   ungroup()
69 survey.geoavg
70
71 #Average biomass over years
72 survey.geotrends = surv_df %>%
73   filter(taxa %in% tax_list) %>%
74   #Sum by haul first
75   group_by(HaulID, year, taxa) %>%
76   summarise(kgkm = sum(DensBiom_kg_Sqkm)) %>%
77   #Take mean over time
78   group_by(taxa, year) %>%
79   summarise(av_kgkm=exp(mean(log(kgkm)))) %>%
80   ungroup()

```

```
81 survey.geotrends
82
83 #Plot average biomass time series
84 p2<- ggplot(survey.geotrends, aes(x=year, y=av_kgkm)) +
85   geom_line(color="grey") +
86   geom_point(color="blue") +
87   facet_wrap(~taxa, scales="free") +
88   theme_minimal(base_size = 9) +
89   theme(axis.text.x = element_text(angle = 45,
90                                     hjust = 1)) +
91   labs(title = "Mean observed biomass",
92        x = "Year",
93        y = "(Geometric) Average biomass density (kg/km^2)")
94 p2
```

C.1 Time Series of Arithmetic Average Biomass Density

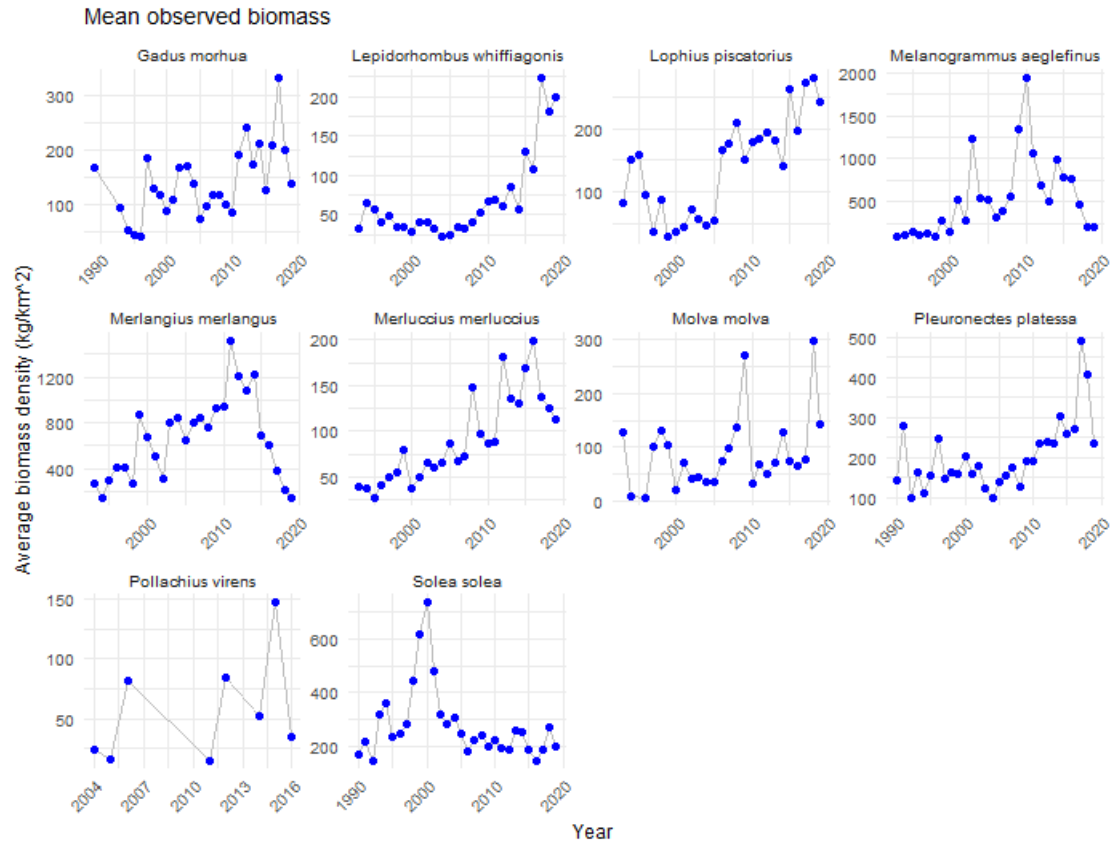


Figure 18: Time series plots for each of our species of interest that show the arithmetic average biomass density over the years; obtained by Cefas survey data.

C.2 Time Series of Geometric Average Biomass Density

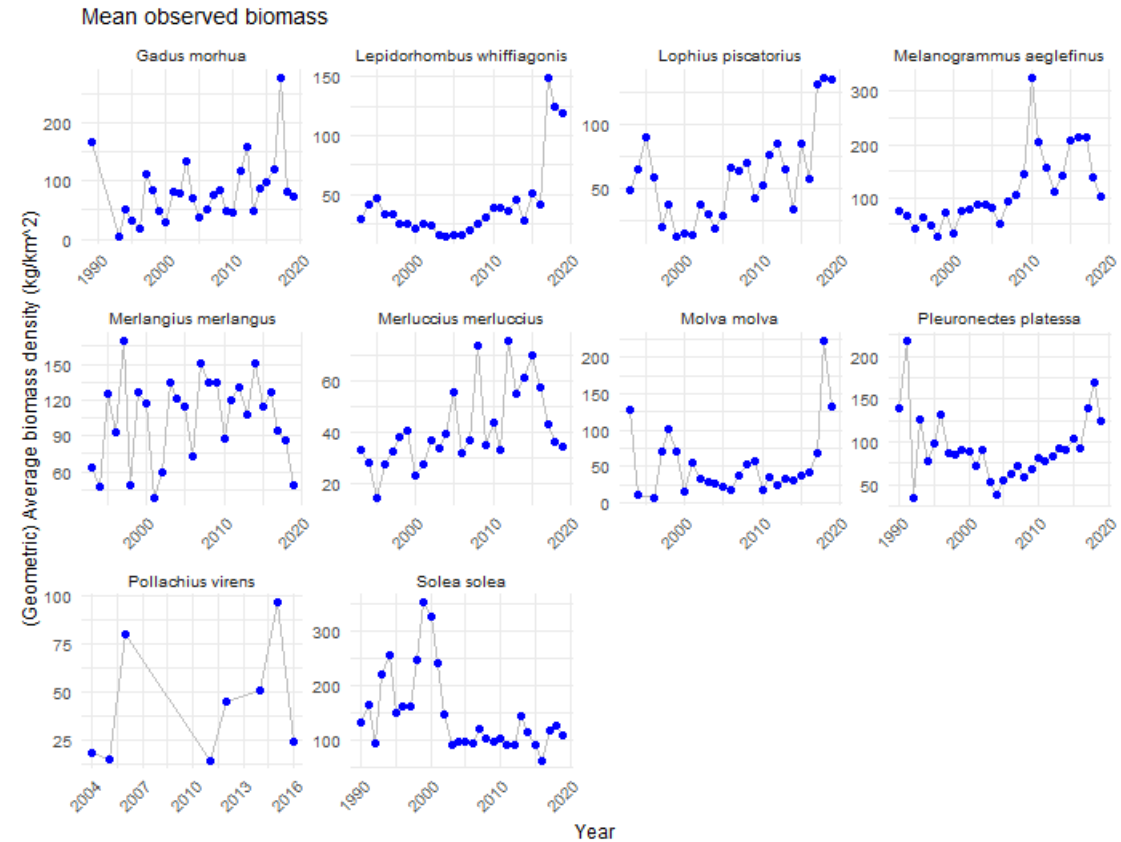


Figure 19: Time series plots for each of our species of interest that show the geometric average biomass density over the years; obtained by Cefas survey data.

C.3 Observed Biomass Parameters using Arithmetic Mean

Taxa	Observed Biomass (kg/km ²)
Gadus morhua	164.147589663092
Lepidorhombus whiffagonis	161.37811170745
Lophius piscatorius	254.568938728212
Melanogrammus aeglefinus	218.03167748774
Merlangius merlangus	184.391048282966
Merluccius merluccius	77.1292410011376
Molva molva	211.306644207336
Pleuronectes platessa	274.490121764717
Pollachius virens	425.0454269831
Solea solea	284.482522126246

Table 3: Table displaying the observed biomass parameters for our species of interest using the arithmetic mean.

D Code to Create a Multispecies Size Spectrum Model using mizer

```

1 #Load necessary R packages
2 library(devtools)
3 install_github("sizespectrum/mizerExperimental")
4 install_github("sizespectrum/mizer")
5 library(dplyr)
6 library(mizer)
7 library(mizerExperimental) #Has some additional features to mizer R package
8 library(ggplot2)
9 library(readxl)

10
11 #Define function that will be used to calculate Balanced Harvesting mortality
12 productionFMort <- function(params, n, effort, e_growth, ...) {
13   usual_f_mort <- colSums(mizerFMortGear(params, effort))
14   production_density <- sweep(e_growth * n, 2, params@w, "*")
15   production_density * usual_f_mort
16 }
17
18 #Define function that adds up yield of all species at each time step
19 TotalYield <- function(sim) {
20   y <- getYield(sim)
21   y_total <- rowSums(y)

```

```

22     return(y_total)
23 }
24
25 #Define function to add up biomass of all species at each time step
26 TotalBiomass <- function(sim) {
27   b <- getBiomass(sim)
28   b_total <- rowSums(b)
29   return(b_total)
30 }
31
32 #Define function the adds up abundance spectrum of all species at each time step
33 TotalAbundance <- function(sim) {
34   n <- getN(sim)
35   n_total <- rowSums(n)
36   return(n_total)
37 }
38
39 Model_params <- read_excel("Model params.xlsx", range = "B2:J12") #Load compiled parameter
→ list into R
40
41 sp <- Model_params #Creates a data frame of the original model parameters
42
43 #Need to rename the variables in the data frame to coincide with how mizer recognises them
44 sp$species <- sp$"Species of interest"
45 sp$w_inf <- sp$W_inf
46 sp$biomass_observed <- sp$"Observed Biomass (kg/km^2)"
47 sp$k_vb <- sp$"Growth coefficient K"
48
49 #Allometric parameters a and b
50 sp$a <- 0.006
51 sp$b <- 3
52 sp$w_mat <- sp$a * sp$L_mat ^ sp$b #Convert length at maturity to weight at maturity
53 sp$w_mat
54
55 #Adding predation parameters
56 Predation_Params <- read_excel("Predation Params.xlsx") #Load predation parameter list
→ into R
57 sp$beta <- Predation_Params$beta
58 sp$sigma <- Predation_Params$sigma
59
60 params <- newMultispeciesParams(sp) #Create parameter object
61
62 #Adding fishing gear parameters

```

```

63 gear_params(params)
64 gear_params(params)$catchability <- sp$`Fishing (external) mortality rate`
65 gear_params(params)$knife_edge_size <- as.numeric(sp$`Minimum landing size (cm)`)
66 gear_params(params)$knife_edge_size[7] <- 29.6 #Choose a value for anglerfish because it
   ↳ has no min landing size
67
68 #Adding interaction matrix
69 Interaction.matrix <- read.delim("Interaction matrix.txt", header=FALSE) #Load interaction
   ↳ matrix into R
70 inter <- as.matrix(Interaction.matrix)
71 rownames(inter) <- sp$`Species of interest`
72 colnames(inter) <- sp$`Species of interest`
73 params <- setInteraction(params, interaction = inter) #Pass interaction matrix to
   ↳ parameter object
74
75 ###Calibrate model to current ecosystem with constant fishing effort at maturity size###
76 params_minlandfishing <- params
77
78 initial_effort(params_minlandfishing) <- 10 #fishing effort
79
80 params_minlandfishing <- steady(params_minlandfishing) #Running dynamics to steady state
81
82 species_params(params) #Outputs table of all the species parameters
83
84 plotSpectra(params_minlandfishing, power=0, resource = FALSE, total = TRUE) #Plots
   ↳ abundance spectrum as a function of size
85 plotSpectra(params_minlandfishing, power=1, resource = FALSE, total = TRUE) #Plots biomass
   ↳ spectrum as a function of size or abundance spectrum as a function of log size
86 plotSpectra(params_minlandfishing, power=2, resource = FALSE, total = TRUE) #Plots biomass
   ↳ as a function of log size aka Sheldon spectrum
87
88 plotBiomassObservedVsModel(params_minlandfishing) #Plots model biomasses against observed
   ↳ biomasses
89 plotGrowthCurves(params_minlandfishing, species_panel = TRUE) #Plots model growth curves
   ↳ against vonB growth curves
90
91 #Opens R shiny gadget to tune growth curves
92 params_minlandfishing <- tuneGrowth(params_minlandfishing)
93
94 #Save updated parameters
95 saveParams(params_minlandfishing, "params_minlandfishing.rds") #Can be accessed via Git
   ↳ repository
96

```

```

97  #To re-create following simulation & plots, load in updated parameters object
98  params_minlandfishing <- readRDS("params_minlandfishing.rds")
99
100 sim1 <- project(params_minlandfishing, effort=10, t_max = 75) #Run simulation for 75 years
101 plot(sim1)
102 plotBiomass(sim1, total = TRUE)
103 plotSpectra(sim1, power=1, resource = FALSE, total = TRUE)
104 slope1 <- getCommunitySlope(sim1, min_w = 0.01, max_w = 1000)
105 mean(slope1$slope) #-0.4367606
106
107 #####No fishing#####
108 params_nofishing <- params_minlandfishing
109 params_nofishing <- steady(params_nofishing) #Re-run dynamics to steady state
110 #zero fishing effort means no fishing in the system
111 sim0 <- project(params_nofishing, effort = 0, t_max = 75) #Run simulation for 75 years
112 plot(sim0)
113 plotBiomass(sim0, total = TRUE)
114 plotSpectra(sim0, power=1, resource = FALSE, total = TRUE)
115 slope0 <- getCommunitySlope(sim0, min_w = 0.01, max_w = 1000)
116 mean(slope0$slope) #-0.8117456
117
118 #Plot relative total abundances by size in the final time step
119 total_abund0 <- colSums(finalN(sim0))
120 total_abund1 <- colSums(finalN(sim1))
121 relative_abundance <- total_abund1/total_abund0
122 plot(x = w(params), y = relative_abundance, log = "xy", type = "n",
123       xlab = "Size [g]", ylab = "Relative abundance")
124 lines(x = w(params), y = relative_abundance)
125 lines(x = c(min(w(params)), max(w(params))), y = c(1, 1), lty = 2)
126
127 #Plot total predation mortality by size for each fishing scenario
128 PMort0 <- getPredMort(params_nofishing, finalN(sim0))[4,]
129 PMort1 <- getPredMort(params_minlandfishing, finalN(sim1))[4,]
130 plot(x = w(params), y = PMort0, log = "x", type = "n",
131       xlab = "Size [g]", ylab = "Predation Mortality [1/year]")
132 lines(x = w(params), y = PMort0, lty = 2)
133 lines(x = w(params), y = PMort1)
134 legend(x="topright", legend = c("no fishing", "fishing"), lty = c(2,1))
135
136 #####Balanced harvesting#####
137 params_BH <- params_minlandfishing
138
139 #Change size selectivity and gear to describe balanced harvesting

```

```

140 params_BH@gear_params$knife_edge_size <-
141   ↪ params_BH@species_params$Minimum.landing.size..cm.
142 params_BH@gear_params$knife_edge_size[7] <- 29.6
143 params_BH@species_params$knife_edge_size <-
144   ↪ params_BH@species_params$Minimum.landing.size..cm.
145 params_BH@species_params$knife_edge_size[7] <- 29.6
146 gear_params(params_BH)$gear <- "balanced"
147 species_params(params_BH)$gear <- "balanced"
148 params_BH <- setRateFunction(params_BH, "FMort", "productionFMort")
149 params_BH <- setFishing(params_BH, initial_effort = 10e4)
150 saveParams(params_BH, "params_BH_beforesteady.rds")
151 params_BH <- steady(params_BH) #Run dynamics to steady state
152 params_BH <- tuneGrowth(params_BH) #Tune parameters then re-run to steady state
153
154 #Save updated parameters
155 saveParams(params_BH, "params_BH.rds") #Can be accessed via Git repository
156
157 #To re-create following simulation & plots, load in updated parameters object
158 params_BH <- readRDS("params_BH.rds")
159
160 simBH <- project(params_BH, effort=10e4, t_max = 75) #Run simulation for 75 years
161 plot(simBH)
162 plotBiomass(simBH, total = TRUE)
163 plotSpectra(simBH, power=1, resource = FALSE, total = TRUE)
164 slopeBH <- getCommunitySlope(simBH, min_w = 0.01, max_w = 1000)
165 mean(slopeBH$slope) #-1.291445
166
167 #Simulate a BH model without running to steady state
168 #To re-create following simulation & plots, load in updated parameters object
169 params_BH2 <- readRDS("params_BH_beforesteady.rds")
170 params_BH2 <- setFishing(params_BH2, initial_effort = 0.1)
171 params_BH2@gear_params$catchability <- 1
172 simBH2 <- project(params_BH2, effort=0.1, t_max = 75) #Run simulation for 75 years
173 plot(simBH2)
174 plotBiomass(simBH2, total = TRUE)
175 plotSpectra(simBH2, power=1, resource = FALSE, total = TRUE)
176 slopeBH2 <- getCommunitySlope(simBH2, min_w = 0.01, max_w = 1000)
177 mean(slopeBH2$slope) #-1.039897
178
179 #Plot total yield for each fishing method over time
180 TotYield1 <- TotalYield(sim1)
181 TotYieldBH <- TotalYield(simBH)
182 matplot(cbind(TotYield1, TotYieldBH),

```

```

181      log = "xy", type = "l", #main = "Total yield of all species over time",
182      xlab = "Year", ylab = "Yield", col = c(2,4), lty=c(1,1),
183      lwd = 3, bty = "l",cex.axis=1.2,cex.lab=1.2)
184 legend(x = "center",legend = c("Constant Fishing at Min Landing Size","Balanced
185   Harvesting"),
186   lty = c(1,1), col = c(2,4), lwd = 3, cex = 1.2, title = "Fishing method")
187
188 TotYieldBH2 <- TotalYield(simBH2)
189 matplot(cbind(TotYield1, TotYieldBH2),
190   log = "xy", type = "l", #main = "Total yield of all species over time",
191   xlab = "Year", ylab = "Yield", col = c(2,4), lty=c(1,1),
192   lwd = 3, bty = "l",cex.axis=1.2,cex.lab=1.2)
193 legend(x = "right",legend = c("Constant Fishing at Min Landing Size","Balanced Harvesting
194   II"),
195   lty = c(1,1), col = c(2,4), lwd = 3, cex = 1, title = "Fishing method")
196
197 #Plot total biomass for each fishing method over time
198 TotBiom1 <- TotalBiomass(sim1)
199 TotBiom0 <- TotalBiomass(sim0)
200 TotBiomBH <- TotalBiomass(simBH)
201 TotBiomBH2 <- TotalBiomass(simBH2)
202 matplot(cbind(TotBiom1, TotBiom0, TotBiomBH, TotAbunBH2),
203   log = "xy", type = "l", main = "Total Biomass",
204   xlab = "Year", ylab = "Biomass [kg km^-2 year^-1]", col = c(2,3,4,1),
205   lty=c(1,1,1),
206   lwd = 3, cex.main=1.2, cex.axis=1.5, cex.lab=1.5)
207 legend(x = "topleft", legend = c("Constant Fishing at Min Landing Size","No
208   Fishing","Balanced Harvesting","Balanced Harvesting II"),
209   lty = c(1,1,1), col = c(2,3,4,1), lwd = 3, cex = 0.7, title = "Fishing method")
210
211 #Just plotting the two fishing systems
212 matplot(cbind(TotBiom1, TotBiomBH),
213   log = "xy", type = "l", main = "Total Biomass",
214   xlab = "Year", ylab = "Biomass [kg km^-2 year^-1]", col = c(2,4), lty=c(1,1),
215   lwd = 3, cex.main=1.2, cex.axis=1.5, cex.lab=1.5)
216 legend(x = "center",legend = c("Constant Fishing at Min Landing Size","Balanced
217   Harvesting"),
218   lty = c(1,1), col = c(2,4), lwd = 3, cex = 1.2, title = "Fishing method")
219
220 matplot(cbind(TotBiom1, TotBiomBH2),
221   log = "xy", type = "l", main = "Total Biomass",
222   xlab = "Year", ylab = "Biomass [kg km^-2 year^-1]", col = c(2,4), lty=c(1,1),
223   lwd = 3, cex.main=1.2, cex.axis=1.5, cex.lab=1.5)

```

```

219 legend(x = "right",legend = c("Constant Fishing at Min Landing Size","Balanced Harvesting
220   ↵ II"),
221     lty = c(1,1), col = c(2,4), lwd = 3, cex = 1, title = "Fishing method")
222
223 #Plot total abundance for each fishing method over time
224 TotAbun1 <- TotalAbundance(sim1)
225 TotAbun0 <- TotalAbundance(sim0)
226 TotAbunBH <- TotalAbundance(simBH)
227 TotAbunBH2 <- TotalAbundance(simBH2)
228 matplot(cbind(TotAbun1, TotAbun0, TotAbunBH, TotAbunBH2),
229   log = "xy", type = "l", main = "Total Abundance",
230   xlab = "Year", ylab = "Abundance", col = c(2,3,4,1), lty=c(1,1,1),
231   lwd = 3, cex.main=1.2, cex.axis=1.5, cex.lab=1.5)
232 legend(x = "topleft",legend = c("Constant Fishing at Min Landing Size","No
233   ↵ Fishing","Balanced Harvesting", "Balanced Harvesting II"),
234     lty = c(1,1,1), col = c(2,3,4,1), lwd = 3, cex = 0.7, title = "Fishing method")
235 mean(TotAbunBH) #47744.72
236 mean(TotAbunBH2) #49755.26
237 min(TotAbun0) #219.0246
238 max(TotAbun0) #10263464886

```

D.1 R Shiny Tuning Parameters Gadget

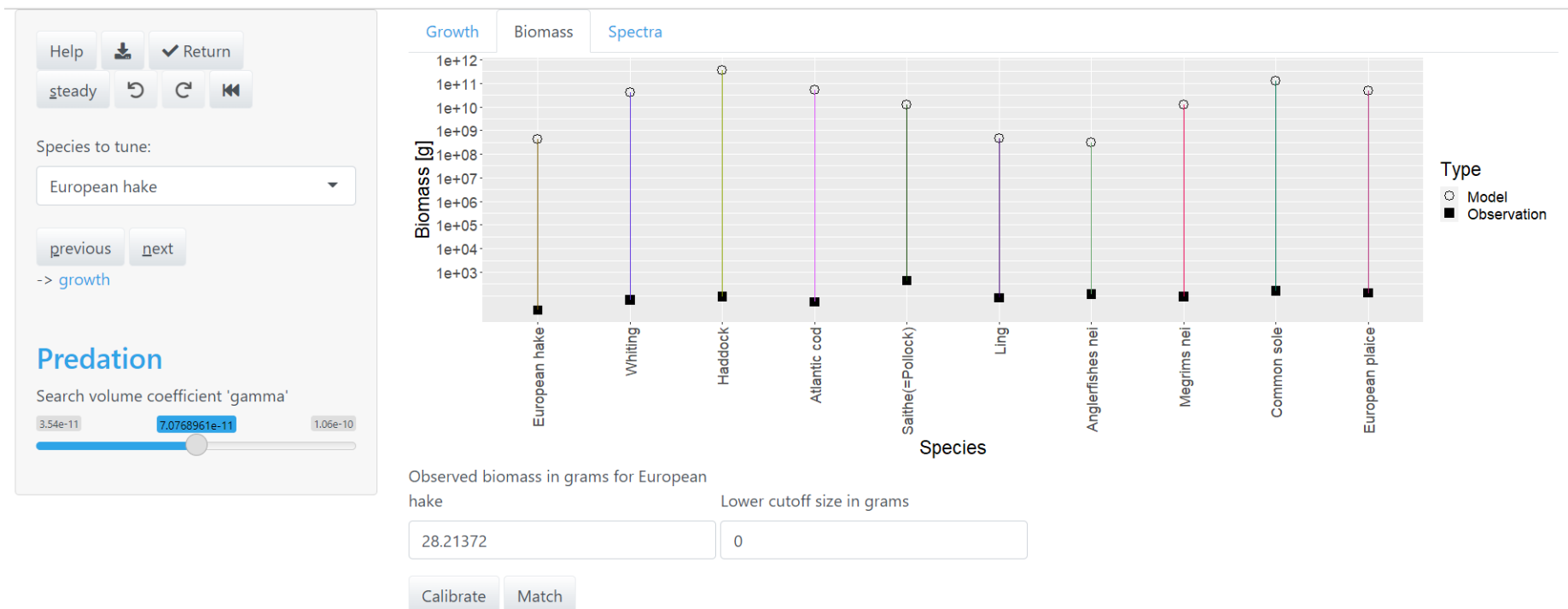


Figure 20: Example of the R shiny gadget interface, which is used to tune model parameters.

D.2 Tuning Growth Curves

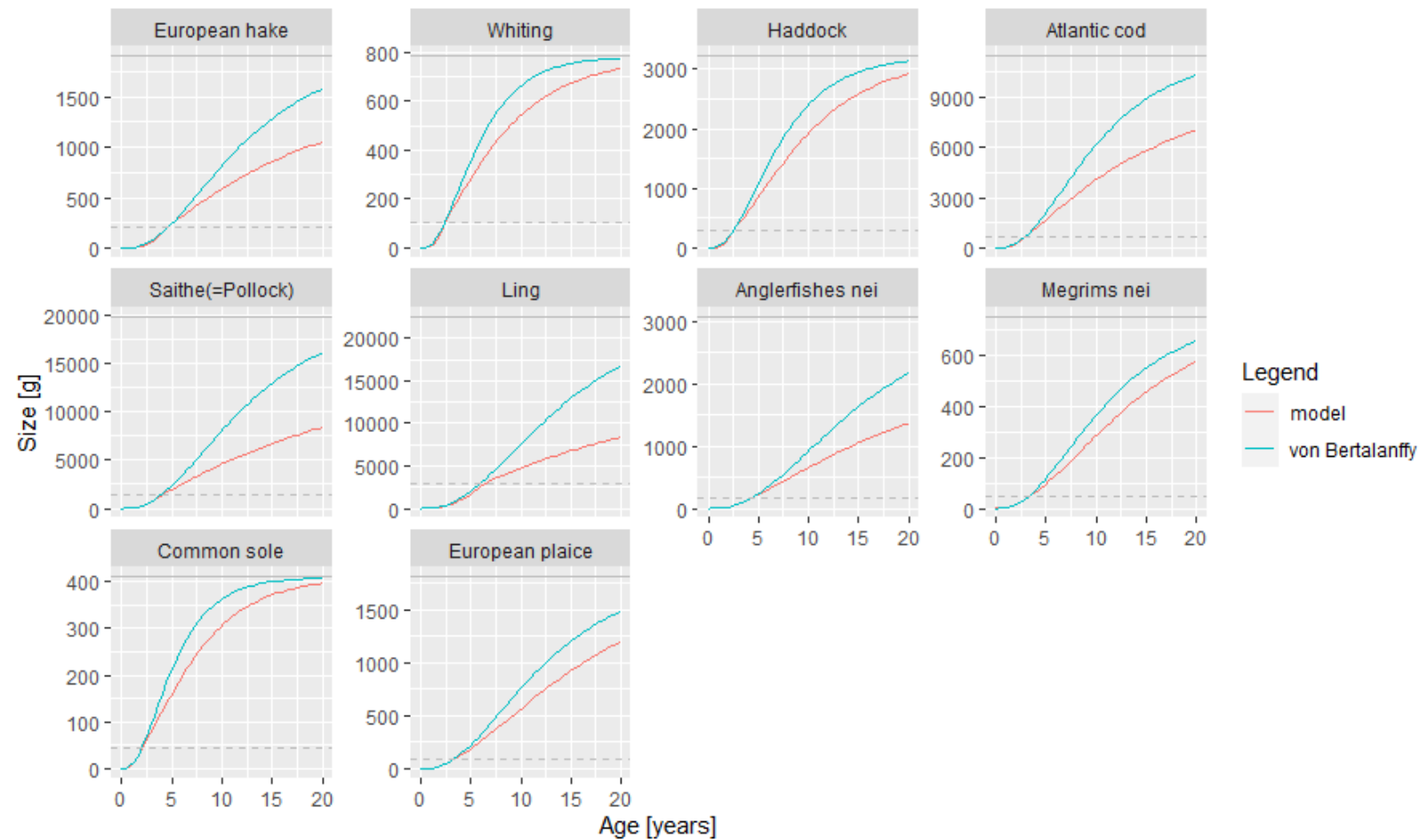


Figure 21: Growth curves for the Southwest marine ecosystem with constant fishing level at minimum landing size before tuning.

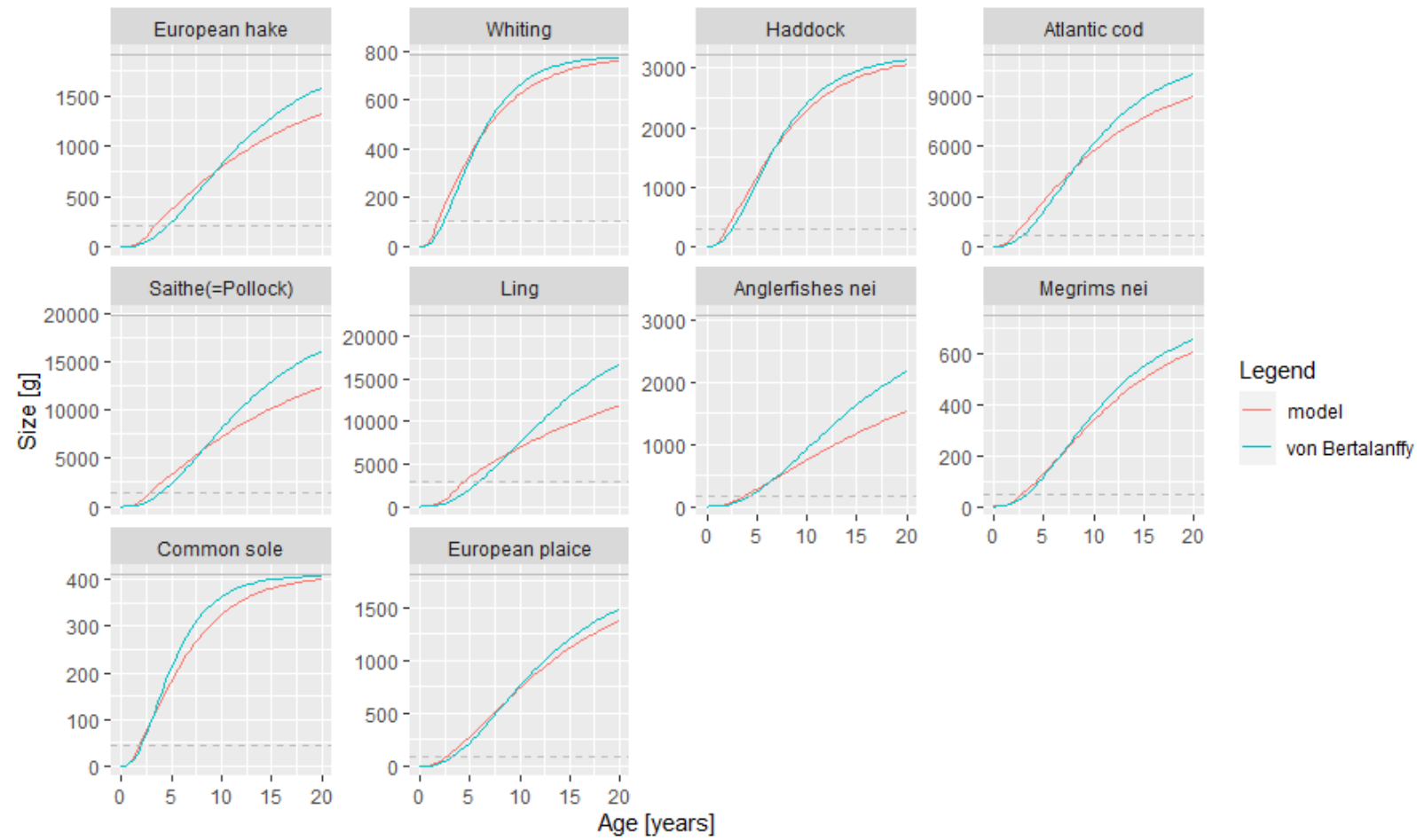


Figure 22: Growth curves for the Southwest marine ecosystem with constant fishing level at minimum landing size after tuning.